

Accepted Manuscript

C-3 Benzoic Acid Derivatives of C-3 Deoxybetulinic Acid and Deoxybetulin as HIV-1 Maturation Inhibitors

Zheng Liu, Jacob J. Swidorski, Beata Nowicka-Sans, Brian Terry, Tricia Protack, Zeyu Lin, Himadri Samanta, Sharon Zhang, Zhufang Li, Dawn D. Parker, Sandhya Rahematpura, Susan Jenkins, Brett R. Beno, Mark Krystal, Nicholas A. Meanwell, Ira B. Dicker, Alicia Regueiro-Ren

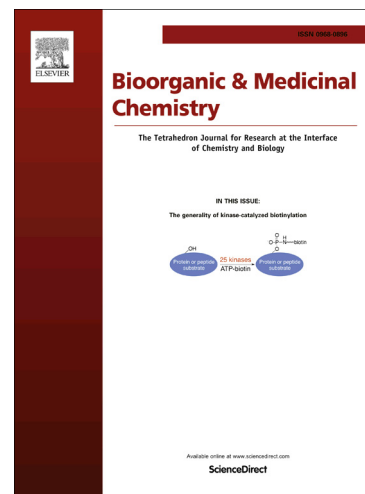
PII: S0968-0896(16)30138-9
DOI: <http://dx.doi.org/10.1016/j.bmc.2016.03.001>
Reference: BMC 12850

To appear in: *Bioorganic & Medicinal Chemistry*

Received Date: 11 January 2016
Revised Date: 21 February 2016
Accepted Date: 1 March 2016

Please cite this article as: Liu, Z., Swidorski, J.J., Nowicka-Sans, B., Terry, B., Protack, T., Lin, Z., Samanta, H., Zhang, S., Li, Z., Parker, D.D., Rahematpura, S., Jenkins, S., Beno, B.R., Krystal, M., Meanwell, N.A., Dicker, I.B., Regueiro-Ren, A., C-3 Benzoic Acid Derivatives of C-3 Deoxybetulinic Acid and Deoxybetulin as HIV-1 Maturation Inhibitors, *Bioorganic & Medicinal Chemistry* (2016), doi: <http://dx.doi.org/10.1016/j.bmc.2016.03.001>

This is a PDF file of an unedited manuscript that has been accepted for publication. As a service to our customers we are providing this early version of the manuscript. The manuscript will undergo copyediting, typesetting, and review of the resulting proof before it is published in its final form. Please note that during the production process errors may be discovered which could affect the content, and all legal disclaimers that apply to the journal pertain.



C-3 Benzoic Acid Derivatives of C-3 Deoxybetulinic Acid and Deoxybetulin as HIV-1 Maturation Inhibitors

Zheng Liu,^{1,*} Jacob J. Swidorski,¹ Beata Nowicka-Sans,² Brian Terry,² Tricia Protack,² Zeyu Lin,² Himadri Samanta,² Sharon Zhang,² Zhufang Li,² Dawn D. Parker,³ Sandhya Rahematpura,³ Susan Jenkins,³ Brett R. Beno,⁴ Mark Krystal,² Nicholas A. Meanwell,¹ Ira B. Dicker,² and Alicia Regueiro-Ren^{1,*}

¹Department of Discovery Chemistry, ²Virology, ³Pharmaceutical Candidate Optimization, ⁴Computer-Assisted Drug Design

Bristol-Myers Squibb Research and Development

5 Research Parkway

Wallingford, CT 06492, USA

ABSTRACT: A series of C-3 phenyl- and heterocycle-substituted derivatives of C-3 deoxybetulinic acid and C-3 deoxybetulin was designed and synthesized as HIV-1 maturation inhibitors (MIs) and evaluated for their antiviral activity and cytotoxicity in cell culture. A 4-substituted benzoic acid moiety was identified as an advantageous replacement for the 3'3'-dimethylsuccinate moiety present in previously disclosed MIs that illuminates new aspects of the topography of the pharmacophore. The new analogs exhibit excellent in vitro antiviral activity against wild-type (wt) virus and a lower serum shift when compared with the prototypical HIV-1 MI bevirimat (**1**, BVM), the first MI to be evaluated in clinical studies. Compound **9a** exhibits comparable cell culture potency toward wt virus as **1** (WT EC₅₀ = 16 nM for **9a** compared to 10 nM for **1**). However, the potency of **9a** is less affected by the presence

of human serum, while the compound displays a similar pharmacokinetic profile in rats to **1**. Hence **9a**, the 4-benzoic acid derivative of deoxybetulinic acid, represents a new starting point from which to explore the design of a 2nd generation MI.

Keywords: HIV-1, maturation inhibitors, betulinic acid, triterpene, antiviral.

INTRODUCTION

Combination antiretroviral therapy (cART) has transformed HIV-1 infection into a more manageable disease for the majority of patients.^{1,2} The combination regimes consist of three antiretroviral drugs that are generally selected from four classes based upon their mechanism of action - nucleoside and nucleotide reverse transcriptase inhibitors, protease inhibitors, and integrase inhibitors, with a fifth class, entry inhibitors, used less frequently.³ However, issues associated with long term toxicity,⁴ therapeutic compliance⁵ and the development of resistance⁶ remain as major causes of treatment failure. In order to address these problems, the discovery of antiretroviral drugs targeting new mechanisms of action (MOAs) with improved safety profiles remains a high priority. Virion maturation is a key step in the virus life cycle and therapeutic intervention at this stage of the replication process has attracted the attention of several groups.⁷⁻¹¹ During this phase of the life cycle, the viral protease cleaves the Gag polyprotein sequentially in five different positions in a process that is carefully choreographed to release the structural proteins MA, CA, NC and p6, as well as two spacer peptides, SP1 and SP2 (Figure 1).¹² The last of the proteolytic cleavages is the rate-limiting step of this process and takes place at the CA-SP1 junction and is the critical step in the maturation of the virion into the conical shape that is characteristic of infectious virus.¹³ Maturation inhibitors (MIs) bind to this segment of the Gag polyprotein, preventing the protease from converting p25 Gag (CA/SP1) to the mature p24 (CA) protein, consequently leading to the production of immature HIV-1 particles which are not infectious.^{12,14,15}

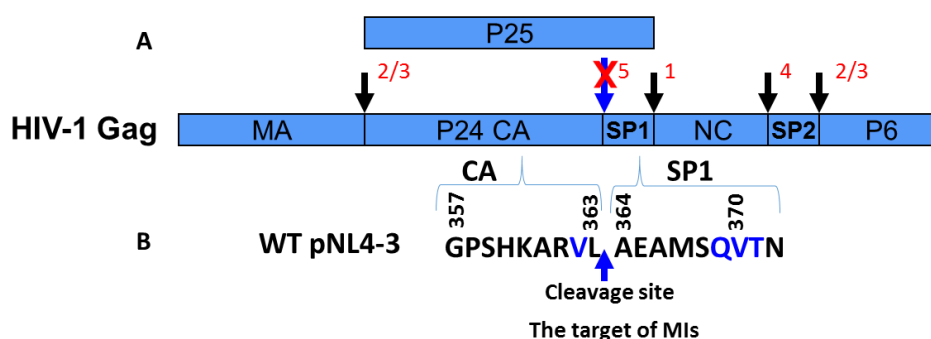
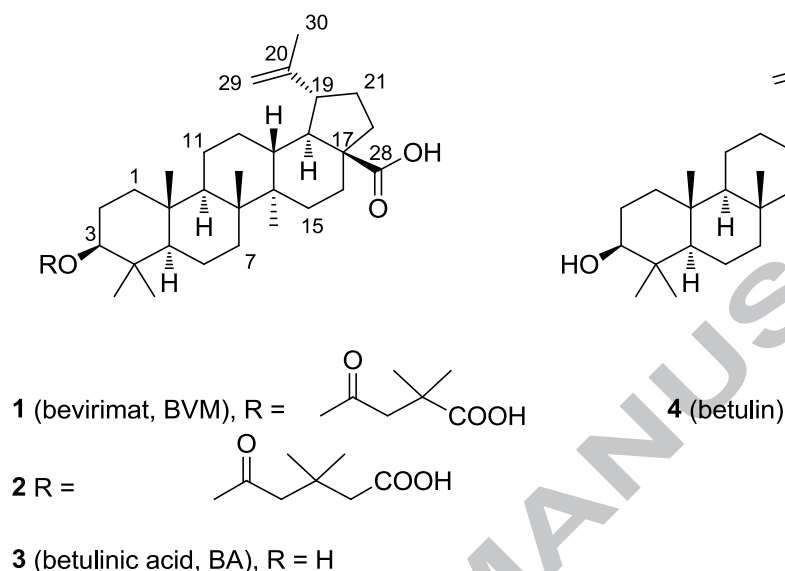


Figure 1. 1a) Protease processing sites within the HIV-1 Gag polyprotein. MIs prevent the last cleavage of p25 Gag (CA/SP1) to the mature p24 (CA). The order of the cleavage events is noted in red. 1b) Amino acid residues in the proximity of the CA/SP1 cleavage site. Amino acid residues that contribute to reduced susceptibility to **1** are marked in blue.

Bevirimat (**1**) was the first MI to be advanced into clinical trials and achieved proof of concept for this MOA by reducing viral load in HIV-1 infected patients.¹⁶ However, subsequent studies in treatment-experienced patients receiving the drug by oral administration for 10 days revealed that only 45% of the subjects responded to therapy.¹⁷ A careful analysis of the data differentiated responders from non-responders based on baseline polymorphisms occurring proximal to the CA/SP1 cleavage site, specifically at residues 362 and 369-371 in the Gag protein.¹⁸ In addition, **1** exhibited high protein binding (>99.9%), which reduced the in vitro antiviral activity by >100-fold, necessitating a high dose in order to achieve clinical efficacy, since target plasma levels were defined as multiples of the protein binding-adjusted EC₅₀ in cell culture.¹⁹ Furthermore, the poor solubility of **1** translated to lower oral exposure than expected as a consequence of solubility- and dissolution-limited absorption,²⁰ further complicating the development path for **1** as an anti-HIV-1 agent, and this compound was eventually abandoned.²¹ These shortcomings provide a clear objective for the pre-clinical profile of a second

generation MI in terms of improved polymorphic virus coverage, reduced protein binding and better pharmaceutical properties.



Structurally, **1** is the 3-*O*-(3',3'-dimethyl succinyl) ester derivative of the natural product betulinic acid (**3**). Although **3** possesses weak anti-HIV-1 activity, it is the dimethyl succinate side chain that decorates the core C-3 hydroxyl group that confers the unique maturation inhibitory activity associated with **1**, exemplified by an EC₅₀ value of 0.35 nM in acutely infected H9 lymphocytes.²² However, in correlation with the clinical results, where the efficacy of **1** was highly diminished in patients with pre-existing variations at Gag positions 369-371 of the SP1 peptide, the in vitro activity of **1** toward the most prevalent polymorphic variant (V370A; ~12.4% of isolates listed in the Los Alamos National Laboratory HIV sequence database) was reduced by more than 100-fold when compared with its potency toward wt virus.²³ More recently, it has been demonstrated that modifications at the C-28 position of **1** can, to some extent, improve polymorphic coverage and protein binding.^{23,24}

In the absence of information on the structure of the MI binding site, extensive work has been directed towards the optimization of the C-3 side chain. The terminal carboxylic acid, proper linker length, *gem*-dimethyl substituent and ester functionality are deemed to be critical for potent inhibition of virus containing the most common QVT sequence at the 369-371 positions.²⁵ The vital importance of the *gem*-dimethyl group and the carboxylic acid moiety for potency points towards a conformational preference for a specific positioning of the carboxylic acid presumably aided, in part, by the Thorpe-Ingold effect.²⁶ The only latitude for structural change that has been described in the literature is with the homologated analog 3-*O*-(3'-dimethyl glutaryl) ester **2** which exhibits an EC₅₀ value of 2.3 nM toward wt virus, 6.5-fold less potent than **1**.²⁷ The rigidity of the triterpenoid core defines the relative spatial disposition between the C-3 acyl side chain and the C-28 functionality, and even minor variations in this distance and vector can result in a significant loss of potency.²⁸

The use of conformationally restricted 3-*O*-acyl derivatives as a means to improve antiviral activity by constraining the position of the C-3 pharmacophore was unsuccessful and resulted in compounds with considerably diminished potency.²⁹ We were interested in exploring the concept of conformational constraint in the context of non-ester-based C-3 side chains, with a view to providing additional illumination of the spatial relationships between the acid moiety and the triterpene core. With the appropriate design, it was anticipated that the positioning of the carboxylic acid could be carefully controlled, potentially leading to improved antiviral and physical properties. In order to place the carboxylic acid at a similar distance from the core as in **1**, the use of a six membered ring spacer directly attached to the C-3 position of BA was considered, with the introduction of a planar phenyl ring as the spacer specifically contemplated as a means of further modulating conformational freedom. Accordingly, we set out to prepare a series of benzoic derivatives of both C-3 deoxybetulinic acid and C3-deoxybetulin, with the objective of identifying a basic platform for the development of second generation MIs that would show equivalent or, possibly, improved coverage of naturally occurring

polymorphisms with reduced protein binding. The results of the first steps of that process are reported herein.³⁰

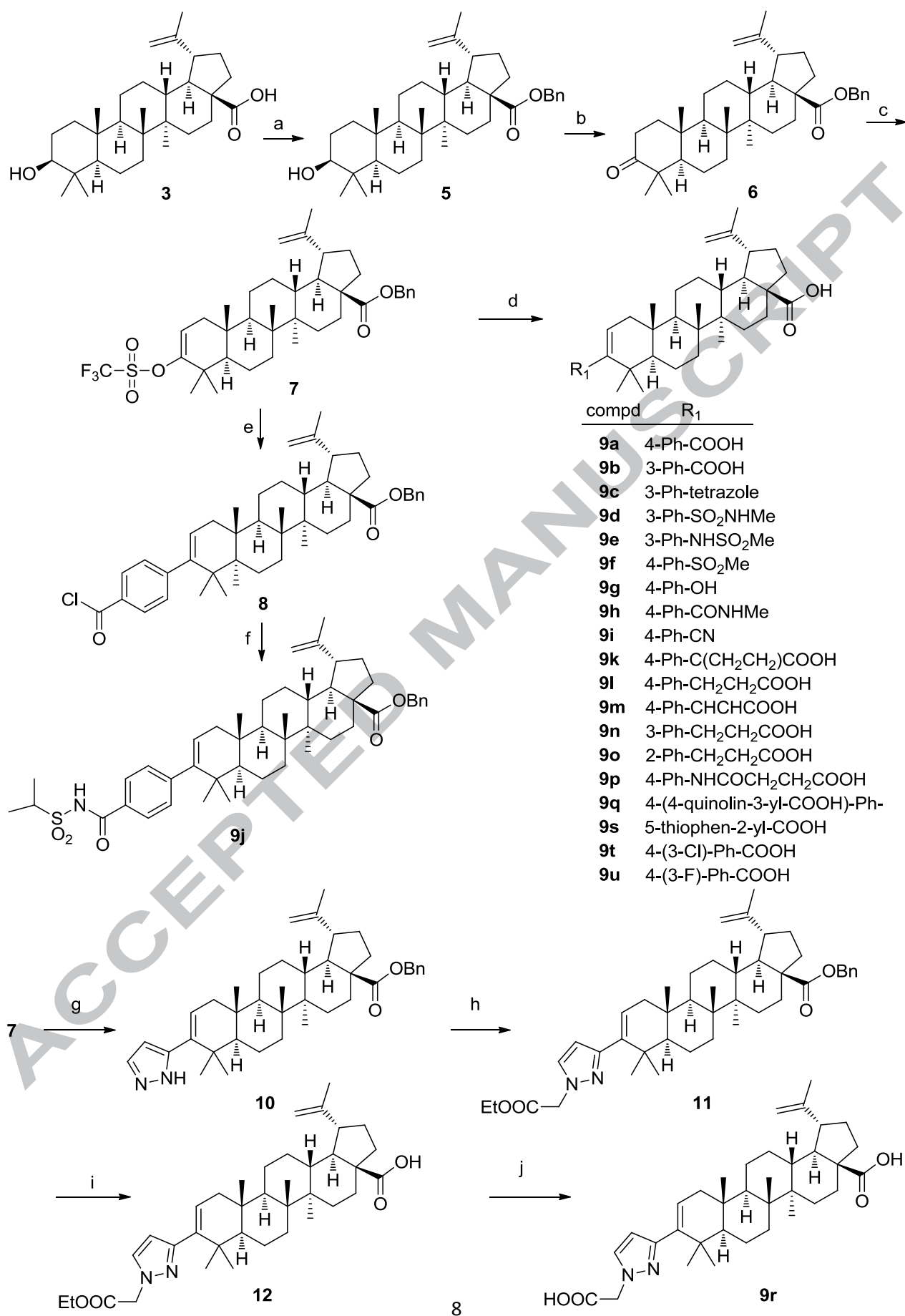
CHEMISTRY

The synthesis of the modified C-3 betulinic acid analogs **9a-9u** that are compiled in Table 1 is outlined in Scheme 1 and began with commercially available betulinic acid.³¹ The C-28 carboxylic acid of **3** was protected with benzyl bromide in the presence of potassium carbonate to give **5**. Oxidation of the hydroxyl group using pyridinium chlorochromate provided ketone **6** which, after treatment with 1,1,1-trifluoro-*N*-phenyl-*N*-(trifluoromethylsulfonyl)methanesulfonamide in the presence of potassium bis(trimethylsilyl)amide at -78°C, afforded the enol triflate **7**, a key intermediate. A Suzuki coupling reaction of **7** with various aryl and heteroaryl boronic acids bearing an unprotected carboxylic acid functionality, provided the corresponding cross-coupled intermediates. Careful control of the catalyst loading (0.1-1 equiv.) and reaction time (1-24 h) facilitated the selective hydrogenolytic removal of the benzyl group with no reduction of the two double bonds present in the core to afford target compounds **9a-9i**, and **9k-9u**.

Alternatively, triflate **7** was reacted with 4-carboxylphenylboronic acid followed by treatment with thionyl chloride to yield the acid chloride **8**. Conversion of **8** to the acylsulfonamide **9j** was accomplished by treatment with the corresponding sulfonamide in the presence of Hunig's base, followed by ester deprotection under the hydrogenolytic conditions described above. The synthesis of **9r** also started from triflate **7** which was subjected to a Suzuki coupling with (1*H*-pyrazol-5-yl)boronic acid to afford the pyrazole derivative **10**. Subsequent alkylation of **10** with ethyl bromoacetate in the presence of potassium carbonate yielded **11** which was selectively debenzylated using triethylamine and *t*-butyldimethylsilane with the help of catalytic amount of palladium acetate to provide **12**. Finally,

hydrolysis of ethyl ester **12** using aqueous NaOH or LiOH as the base generated **9r**. It should be noted that this route was initially approached using the C-28 methyl ester derivative instead of the benzyl ester; however, the final unmasking of the carboxylic acid required harsh conditions (microwave at 240°C/8 h or heating 100°C/2 days) that resulted in loss of material and/or poor yields. The use of a benzyl ester as the protecting group allowed for milder reaction conditions for removal and more convenient workups which led to improved yields.

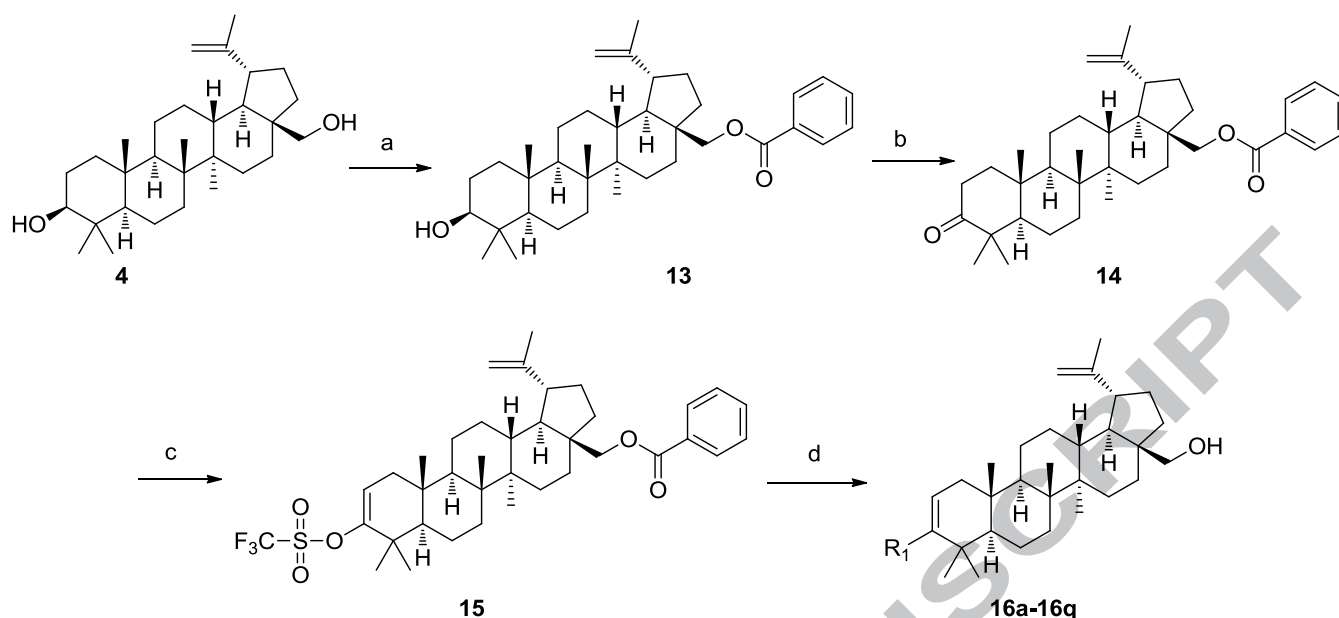
Scheme 1. Synthesis of C-3 deoxybetulinic acid derivatives **9a-9u**.



Reagents and conditions: (a) K_2CO_3 , BnBr, 60°C, 3.5 h, 97%; (b) PCC, CH_2Cl_2 , 15 h, 98%; (c) KHMDS, $PhNTf_2$, THF, -78°C, 1 h, 86%; (d) (i) $R_1-B(OH)_2$, Na_2CO_3 , $Pd(Ph_3P)_4$, DME, H_2O , 100°C, 1.5-3 h. (ii) Pd/C , H_2 , 1 atm, EtOAc, MeOH, rt 3-24 h, 2-52% over two steps; (e) (i) (4-PhCOOH)- $B(OH)_2$, Na_2CO_3 , $Pd(PPh_3)_4$, DME, H_2O , 100°C, 2 h (ii) $SOCl_2$, CH_2Cl_2 , reflux, 17 h, 41% over two steps; (f) (i) RSO_2NH_2 , DMAP, Hunig's Base, DME, rt, 16 h. (ii) 10% Pd/C , H_2 , 40 psi, EtOAc, MeOH, rt., 17 h, 7-26% over two steps; (g) 1*H*-pyrazol-5-ylboronic acid, $Pd(PPh_3)_4$, $Na_2CO_3 \cdot H_2O$, dioxane, water, 85°C, 5.5 h, 61%; (h) $BrCH_2COOEt$, K_2CO_3 , DMF, 75°C, 17 h, 73%; (i) TBDMSH, $Pd(OAc)_2$, TEA, DCE, 60°C, 7.7 h, 55%; (j) NaOH, 1,4-dioxane, 85°C, 17.5 h, 77%.

The C-3 deoxybetulin analogs **16a-16q** were prepared in a similar manner, as outlined in Scheme 2. Betulin (**4**) was used as the starting material and the C-28 primary hydroxyl group was protected using benzoic anhydride to afford ester **13**. Preparation of triflate **15** followed by Suzuki coupling with either aryl carboxylic acid or ester boronic acids or a Stille coupling reaction was performed as described above for the betulinic acid analogs. Ultimately, removal of the benzoyl protecting group in the C-28 position and hydrolysis of the aryl esters, when present, were accomplished in one step using LiOH or NaOH in a mixture of dioxane/water to yield the corresponding target C-28 alcohols **16a-16q** (Table 1). The yields for the reactions described in Schemes 1 and 2 were not optimized.

Scheme 2. Synthesis C-3 deoxybetulin derivatives **16a-16q**.



compd	R ₁	compd	R ₁	compd	R ₁
16a	4-Ph-COOH	16g	5-1 <i>H</i> -pyrazol-3-yl-COOH	16m	4-(3-OMe)-Ph-COOH
16b	4-Ph-tetrazole	16h	3-isoxazol-5-yl-COOH	16n	3,4-Ph-COOH
16c	4-Ph-NHSO ₂ Me	16i	5-thiophen-3-yl-COOH	16o	4-(2-F)-Ph-COOH
16d	4-Ph-NO ₂	16j	4-(3-Cl)-Ph-COOH	16p	4-(2-Cl)-Ph-COOH
16e	2-pyrimidin-5-yl-COOH	16k	4-(3-F)-Ph-COOH	16q	4-(2-Me)-Ph-COOH
16f	5-pyridin-2-yl-COOH	16l	4-(3-OH)-Ph-COOH		

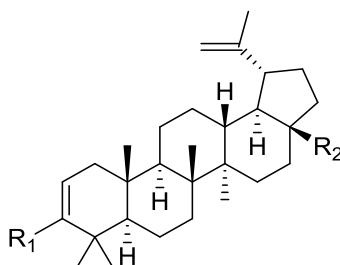
Reagents and conditions: (a) (PhCO)₂O, DMAP, pyridine, 60°C, 3 h; (b) PCC, CH₂Cl₂, rt, 2 h; (c) KHMDS, PhNTf₂, THF, -78°C, 2 h, 60% over 3 steps; (d) (i) R₁-B(OH)₂, Na₂CO₃, K₂CO₃ or K₃PO₄, Pd(PPh₃)₄, dioxane or DME, H₂O, 85°C-100°C, 3-24 h; (ii) LiOH or NaOH, dioxane, H₂O, 75°C, 3-15 h, 2-38% over 2 steps or (i) R₁-SnBu₃, LiCl, Pd(Ph₃P)₄, dioxane, 85°C, 15.5 h; (ii) LiOH or NaOH, dioxane, H₂O, 3.5-18 h, 6-47% over 2 steps.

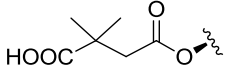
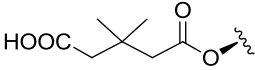
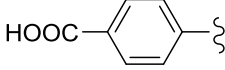
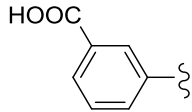
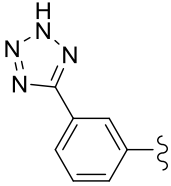
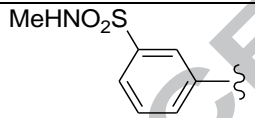
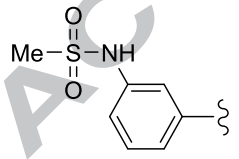
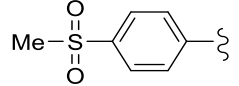
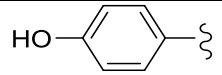
RESULTS AND DISCUSSION

The in vitro antiviral activity and cytotoxicity associated with the target compounds are assembled in Table 1. The C-3 modified betulinic acid and betulin analogs were tested for inhibitory activity toward wt HIV-1 infection in a multiple cycle assay in MT-2 cells using variants of the NLRepRlucP373S virus, an engineered laboratory strain derived from NL₄₋₃ that expresses the *Renilla*

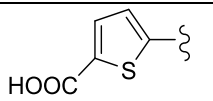
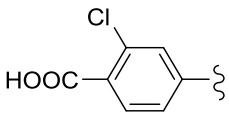
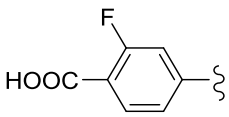
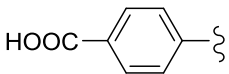
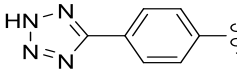
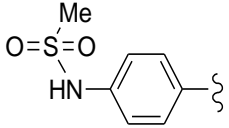
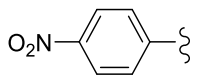
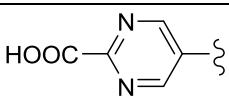
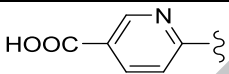
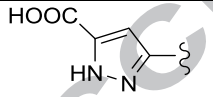
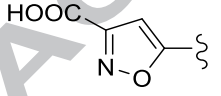
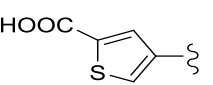
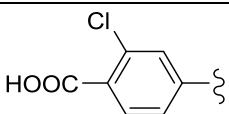
luciferase gene for use as a marker for virus growth. The effect of human serum albumin on compound potency was measured by comparison of inhibitory activities using NLRepRlucP373S virus-infected MT-2 cells in 10% fetal bovine serum (FBS) to that determined using 10% FBS plus 15 mg/mL human serum albumin (HSA). In complete media (10% FBS + 40% human serum + 27 mg/mL HSA), which more closely matches the physiological concentration of HSA (45 mg/mL), the EC_{50} value for **9a** was only 2-fold higher (0.31 μ M), when compared to that in 15 mg/mL HSA. Therefore, 15 mg/mL HSA was used as the screening paradigm to rank the effects of the most important serum component (albumin) shown to reduce the antiviral activity of **1** in serum.³² The ratio between the cell culture potency towards wt virus in the presence and absence of human serum is noted in Table 1 as fold-change WT (HSA) EC_{50} / WT EC_{50} . The V370A virus, which encodes reduced susceptibility to **1**, was identical to the wild type virus except for this single amino acid substitution and represents the most common polymorphic variation in subtype B HIV-1 at position 370 in the Gag protein (~12.4%).³³ The cytotoxicity of the compounds was determined in parallel in MT-2 cells using a redox dye assay (3-(4,5-dimethylthiazol-2-yl)-5-(3-carboxymethoxyphenyl)-2-(4-sulfophenyl)-2H-tetrazolium) with data reported as the half maximal concentration associated with cell viability.³⁴

Table 1. Antiviral activity and cytotoxicity for compounds **1**, **2**, **9a-9u** and **16a-16q**



ACCEPTED MANUSCRIPT							
	R₁	R₂	WT HIV-1 inhibition EC₅₀ (μM)^a	inhibition in the presence of 15 mg/mL HSA EC₅₀ (μM)^a	Fold change EC₅₀ WT(HSA) / EC₅₀ WT	V370A HIV-1 inhibition EC₅₀ (μM)^a	CC₅₀ (μM)^a
1		COOH	0.010±0.011 (n = 69) ^a	0.974±0.71 (n = 15) ^a	97.4	0.553±0.633 (n = 34) ^a	16.8
2		COOH	0.004	0.909	227	-	4.25
9a		COOH	0.016±0.013 (n = 25) ^a	0.150±0.099 (n = 4) ^a	9.4	0.233±0.305 (n = 10) ^a	27.2
9b		COOH	>8	-	-	-	13.8
9c		COOH	>8	-	-	-	10.5
9d		COOH	1.23	-	-	-	13
9e		COOH	2.13	-	-	-	12.7
9f		COOH	2.52	-	-	-	9.72
9g		COOH	0.308	>8	-	-	13.4

9h		COOH	1.60	-	-	-	22.6
9i		COOH	>1.60	-	-	-	4.45
9j		COOH	0.124	0.275	2.2	0.937	8.68
9k		COOH	0.215±0.257 (n = 4) ^a	-	-	0.633	>8
9l		COOH	0.682	-	-	-	6.55
9m		COOH	0.734	-	-	-	>8.0
9n		COOH	0.571	-	-	-	1.83
9o		COOH	3.2	-	-	-	5.03
9p		COOH	1.47	-	-	1.57	7.73
9q		COOH	3.6	-	-	-	15.9
9r		COOH	0.167	-	-	>3	>30

9s		COOH	0.059	-	-	>2	0.79
9t		COOH	0.021±0.025 (n = 5) ^a	0.331	15	0.589	3.08
9u		COOH	0.018±0.023 (n = 5) ^a	0.067	3.7	0.036	10.1
16a		CH ₂ OH	0.011±0.007 (n = 12) ^a	0.027±0.011 (n = 8) ^a	2.5	0.212±0.177 (n = 8) ^a	9.65
16b		CH ₂ OH	3.4	-	-	>4.0	34.3
16c		CH ₂ OH	>1.6	>1.6	-	>1.6	8.82
16d		CH ₂ OH	>4	>4	-	>4	20
16e		CH ₂ OH	1.08	1.08	1	>4	22.3
16f		CH ₂ OH	0.503	-	-	>2	4.30
16g		CH ₂ OH	0.061	-	-	0.348	0.57
16h		CH ₂ OH	0.039	0.295	7.5	>2	12.1
16i		CH ₂ OH	0.38±0.035 (n = 4) ^a	-	-	>2	14.1
16j		CH ₂ OH	0.024	0.094	3.9	0.262	1.97

16k		CH ₂ OH	0.046	0.185	4	0.309	18.8
16l		CH ₂ OH	0.081	0.065	0.8	2.78	9.76
16m		CH ₂ OH	0.513	1.186	2.3	>4	28.7
16n		CH ₂ OH	0.038	-	-	0.212	>20
16o		CH ₂ OH	0.055	0.050	1	1.4	16.5
16p		CH ₂ OH	0.114	0.117	1	>4	17.3
16q		CH ₂ OH	0.613	0.660	1	3.88	7.02

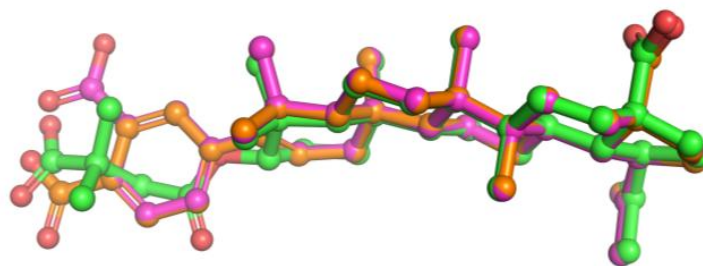
^aThe data provided are the means of at least triplicate values with a mean CV (confidence value) of 83 +/- 50 % for all of the experiments, and all CV values <200 %. Where experiments were performed 4 or more times, the corresponding standard deviations are noted.

We first elected to prepare the 4-benzoic acid **9a** and the 3-benzoic acid **9b** derivatives, which seemed to offer a good approximation of the spatial disposition for the carboxylic acid group when compared with the conformationally more flexible dimethylsuccinate side chain of **1**. Preparation of the 2-benzoic acid analog was not considered at this time for that reason and also because that topological relationship afforded poorly active compounds when examined in the context of saturated ring

systems.²⁹ Compound **9a** exhibited excellent cell culture potency toward the wt virus with an $EC_{50} = 16$ nM, comparable to that of **1**, which demonstrated an $EC_{50} = 10$ nM. However, in the presence of human serum, **9a** was 6.5-fold more potent than **1**, reflective of a much reduced serum binding, (9.4-fold for **9a** compared to 129-fold for **1**).³² Remarkably, the 3-benzoic analog **9b** was over 450-fold less active as an inhibitor of wt virus when compared with **9a**, demonstrating the critical importance of the topographical disposition of the carboxylic acid moiety with respect to the core in the context of this kind of conformational constraint.

An overlay of compounds **1**, **9a**, and **9b** is depicted in Figure 2. The model was generated from low energy conformers identified via conformational searches performed using BatchMin (Version 9.6, Schrödinger, LLC), the OPLS_2005 force-field, and an implicit water solvation model.³⁵ The lowest energy conformer of **9a**, a potent antiviral agent in which the disposition of the carboxylate with respect to the core is the most restricted, was used for fitting conformers of **1** and **9b** based on molecular shape and pharmacophore features. The energy of the conformer of **1** included in the model was < 0.2 kcal/mol above that of the lowest energy conformer identified for the compound. The conformer of **9a** shown is the lowest energy conformer found. In both **9a** and **9b**, the aromatic ring and the triterpenoid core show an almost perpendicular disposition, induced in part by the adjacent *gem*-dimethyl group in the A-ring of the core. The dimethylsuccinate side chain of **1** and the 4-benzoic acid of **9a** overlap quite well to project the respective carboxylic acid moieties in very close spatial proximity. However, in the 3-substituted analog **9b**, the carboxylic acid is clearly displaced and could not readily overlap with the carboxylic acid of **1**. Although no structural information regarding how **1** or any other MI specifically interacts with the binding determinants of the assembled Gag polyprotein is available, these results complement previous reports regarding the importance of the precise location of the carboxylic acid in order to achieve antiviral potency, while providing a more definitive understanding of the topographical relationship with the core.²⁷

Figure 2. Overlay of compounds **1** (green), **9a** (orange), and **9b** (magenta).^a



^aImage generated with the PyMOL Molecular Graphics System (Version 1.7.6, Schrödinger, LLC).

The 4-benzoic acid deoxy-betulin analog **16a** exhibited comparable antiviral potency toward wt and V370A viruses as those of its BA analog **9a**, while in the presence of HSA **16a** was 3-fold more potent than **9a**. Therefore, both C-17 acids (**9**) and C-28 alcohols (**16**) were used as vehicles to further explore the SAR associated with novel C-3 side chains, with some elements of the survey restricted to one or the other chemotype based on synthetic accessibility. In the initial step of this survey, a variety of functionalities that replaced the carboxylic acid moiety in either the 3- or 4-position of the phenyl ring were explored in the context of compounds **9c-9j** and **16b-16d**. It has been shown that under some circumstances, tetrazoles are effective acid isosteres, since they are ionized at physiological pH and maintain a planar topology similar to a carboxylic acid.³⁶ Although this heterocycle is larger than a simple carboxylic acid,^{36c,d} we anticipated it might be an acceptable substitute since the 3-*O*-(3'-dimethyl glutaryl) ester homologue **2** shows similar potency to **1**. However, **16b** showed a significant loss of antiviral potency, while deployment of a tetrazole at C-3 (**9c**) failed to improve upon **9b**, demonstrating that this kind of bioisosterism is sensitive to context. Similarly, analogs incorporating other potential acid isosteres, such as sulfonamides **9d**, **9e** and **16c** and nitro-derivative **16d**, were also

much less potent than the corresponding carboxylic acids.^{36,37} Only phenol **9g** and acylsulfonamide **9j** maintained sub-micromolar inhibitory potency towards wt virus, but these were 18- and 7-fold less potent than **9a** against the wt virus, respectively.^{36,38} Of the acid isosteres examined, the acylsulfonamide **9j** offered the best profile towards wt virus. Perhaps not surprisingly, given the absence of overt acidic functionality, both amide **9h** and nitrile **9i** were also less potent antiviral agents.

The effect of a spacer between the phenyl ring and the carboxylic acid was probed by introducing linkers with different lengths and degrees of flexibility designed to map out a range of topographical opportunity, as exemplified by analogs **9k-9q**. The results revealed a substantial loss of potency with this series, with only **9k-9m**, which incorporate the shortest side chains and most closely resemble the positioning of the carboxylic acid relative to **9a**, displaying sub-micromolar inhibitory potencies. The effect of replacement of the phenyl ring with a series of 5- and 6-membered heterocycles was explored since these present vectors that probe additional topological relationships, a survey represented by analogs **16e-16i** and **9r-9s**. Interestingly, the six-membered ring heterocyclic analogs **16e** and **16f** showed considerably weaker antiviral activity ($EC_{50} > 0.5 \mu M$) toward the wt virus than compounds **9r**, **9s** and **16g-16i** which incorporate five-membered ring heterocycles. Isoxazole **16h** and pyrazole **9r** offered the best profile within this series, exhibiting EC_{50} values of 39 nM and 167 nM, respectively, toward wt virus with cytotoxicities comparable to that of **9a**. Both, pyrazole **16g** and thiazole **9s** appeared to very potent against wt virus, with EC_{50} values of 61 and 59 nM, respectively, but these compounds had low therapeutic indices (EC_{50}/CC_{50}), which casts doubt on the authenticity of the antiviral effect.

Consequently, attention returned to the 4-benzoic acid analogs **9a** and **16a** and the SARs were further explored by introducing substituents at positions 2 and 3 of the phenyl ring. These modifications were designed to influence conformational relationships between the aromatic ring and the core, as well as the carboxylic acid and the phenyl ring. Substitution *meta*- to the carboxylic acid moiety, exemplified

by compounds **16o-16q**, resulted in reduced antiviral potency toward the wt virus, with the EC₅₀ values inversely correlated with the size of the substituent, such that the larger the substituent, the lower the potency. This result seems to indicate that the orientation of the phenyl ring with respect to the core may be affected by steric interactions between the *meta*-substituent and the A-ring *gem*-dimethyl moiety, resulting in a preferred conformation that inadequately complements the binding site. While the smaller *meta*-F, which has an A-value = 0.15, would allow the phenyl ring to adopt an angle with regard to the core that resembles more closely that observed in Figure 2 for **9a**, the larger Cl and Me substituents, with A-values = 0.43 and 1.7, respectively, are forecasted to have larger steric effects that might distort the orientation of the ring to a more perpendicular disposition with respect to the core, which presumably is detrimental for potency.³⁹

Substitution *ortho*- to the carboxylic acid, as in **9t-9u** and **16j-16n**, was better tolerated. The *ortho*-F substituted compound **9u** showed similar antiviral activity toward wt virus as **9a**. However, the effect of the *ortho*-F substitution did not translate to the alcohol series, as illustrated by compound **16k**, which is 4-fold weaker than **16a** toward wt virus. The *ortho*-Cl analogs **9t** and **16j** maintained the antiviral activity of the prototypes **9a** and **16a**, respectively. Introduction of other substituents in the *ortho*-position, including hydroxyl (**16l**) and methoxy (**16m**), further diminished potency. Interestingly, a second carboxylic acid was remarkably well tolerated, as **16n** is just 3-fold weaker than **16a** toward the wt screening virus.

In addition to **9a** and **16a**, select compounds were tested for inhibitory potency toward wt virus in the presence of HSA and the results compiled in Table 1. Phenol **9g** experienced more than a 4-fold serum shift, while the potency of the acylsulfonamide **9j** was shifted by just 2-fold. Isoxazole **16h** experienced a similar serum shift (7.5-fold) to **9a**, while pyrimidine **16e** displayed no change in potency in the presence of HSA. The serum shift for the *ortho*-F analogs **9u** and **16k** was the same (4-fold), while the *ortho*-Cl compounds **9t** and **16j** exhibited a serum shift of 15- and 4-fold, respectively,

recapitulating the larger serum shift associated with the betulinic acid analog than the betulin analogs, observed for **9a** and **16a**. Within the betulin series, the *ortho*- analogs **16j** and **16k** displayed a 4-fold larger serum shift than the corresponding *meta*- analogs **16o** and **16p**, neither of which suffered a loss of potency in the presence of HSA. Thus, for this series of C-3 benzoic acid derivatives the effect of serum is generally modest and less than that observed for **1**.

In terms of activity toward the highly prevalent BVM-resistant polymorphism, V370A, the EC₅₀s of **9a** and **16a** were both = 0.2 μ M, only slightly improved compared to **1**, EC₅₀ = 0.55 μ M. None of the modifications introduced into **9a** explored in analogs **9j-9k**, **9p**, **9r-t**, **16b-16i**, **16l-16q** significantly affected the potency toward the V370A polymorphic virus. Only the *ortho*-F analog **9u** showed better potency than **9a**, although in the betulin series the same modification (**16k**) resulted in a loss of potency when compared with **16a**. Notably, in both cases, this modification adversely affected the solubility of the compounds, making them sufficiently difficult to formulate that they could not be evaluated in vivo to determine their pharmacokinetic profile.

The mechanism of the antiviral activity of **9a** was studied to allow a comparison with **1**. To that end, **9a** was evaluated in an in vitro assay designed to assess inhibition of the final step of CA/SP1 Gag cleavage, which results in the conversion of the capsid precursor protein p25 to the capsid protein p24, concomitant with the release of the SP1 spacer peptide,⁴⁰ the final and key step in the triggering of HIV-1 maturation.⁴¹ Assembled HIV-1 viral-like particles (VLPs) produced in HEK 293T cells using an optimized codon expression vector (1_pcDNAGagOpt) and the VLPs were used as a substrate for in vitro HIV-1 protease cleavage of p25 capsid/spacer peptide 1 (CA/SP1).⁴² As shown in the Western blot in Figure 3, **9a** at 2 μ M (lane 10) inhibits p24 production by 1.6-fold, compared with an average value of 1.6-fold for **1** at 3 and 1 μ M (lanes 3 and 4, respectively), consistent with the assignment of **9a** as an HIV-1 maturation inhibitor specific for the inhibition of p25 cleavage. Analysis of the entire Western

blot (supplementary Figure 1) shows that **9a** is specific for inhibiting p25 cleavage into p24, as there was no indication of inhibition of cleavage at any other sites of the protein.

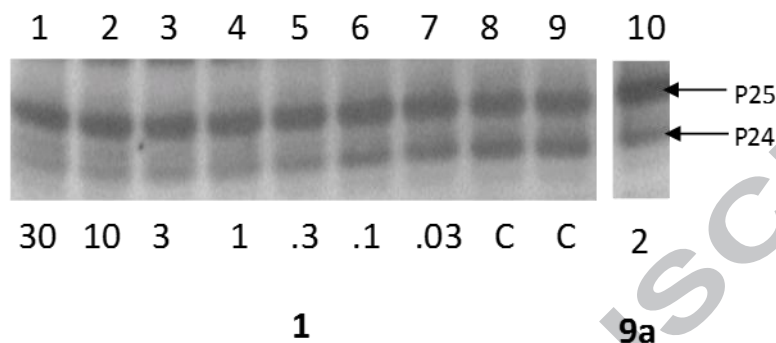


Figure 3. Inhibition of HIV-1 CA-SP1 processing by **1** and **9a**. Lanes are numbered 1-8 (top). Compound **1** was tested at 30 through 0.03 μM (3-fold dilutions, lanes 1-8); compound **9a** was tested at 2 μM (lane 10); C (control, lanes 8 and 9) show samples with buffer only control added. All samples were run on the identical gel, but lane 10 is offset from the others in the Figure due to gel effects.

Additionally, **9a** was evaluated in a competitive binding assay. This assay measures the ability of a target compound to compete with a radiolabeled derivative of **1** (the [³H]-dihydro **1**)⁴³ for binding to purified VLPs. The results show that **9a** binds competitively to wt VLPs with an IC₅₀ of 27 nM (Figure 4).

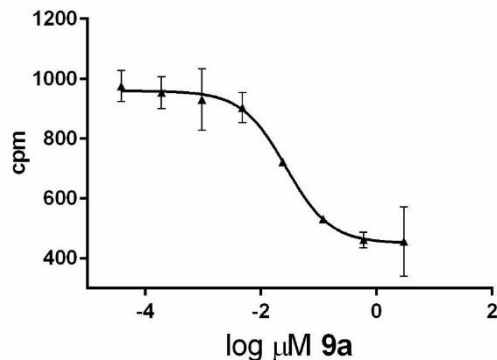


Figure 4. Competitive binding of **9a** to wt VLPs as measured by displacement of [^3H]-dihydro **1**.

The betulinic acid-derived analog **9a** and the betulin-derived analog **16a** were advanced into in vitro assays designed to forecast ADME (absorption, distribution, metabolism and excretion) properties. Both **9a** and **16a** are predicted to be low clearance compounds in the rat and in humans based on their stability upon incubation with rat and human liver microsomes in the presence of NADPH ($t_{1/2} > 120$ min for both compounds in both species). An in vitro assessment of membrane permeability could not be conducted due to the low solubility of these compounds. Nevertheless, both **9a** and **16a** were selected for in vivo pharmacokinetic evaluation in snapshot experiments conducted in rats where comparison was made with **1** as the reference standard. The results are presented in Table 2.

Table 2. In vivo pharmacokinetic properties of compounds **1**, **9a** and **16a** in rats.^a

Cmpd	F(%)	AUC 6h (nM*hr) ^b	C _{max} (nM) ^b	t _{max} (h)	CL	Vss IV (L/Kg)
					iIV(mL/min/kg)	
1	18	6,390	2,587	0.3	4.0	0.1
9a	4	5,724	1,314	4	1.0	0.2
16a	4	2,136	590	5	2.1	0.5

^a Vehicle: polyethylene glycol 300 (PEG 300), ethanol and tween-80 (TW80)(89:10:1 v/v/v), n=2;
Dose 5 mg/kg PO; 1 mg/kg iv; ^b Oral C_{max} and AUC adjusted to 5 mg/kg

In the rat PK study, **9a** displayed lower clearance (1.0 vs. 4.0 mL/min/kg), a smaller volume of distribution (Vss = 0.1 vs. 0.2) and a longer t_{max} (4 vs. 0.3 h) when compared to **1**. The oral exposure of both compounds was comparable (AUC = 5,724 vs. 6,390 nM*hr), although **9a** had lower oral bioavailability (F= 4% compared to 18% for **1**). In contrast, the less polar betulin-based derivative **16a** demonstrated improved clearance (2.1 mL/min/kg) compared to **1** but lower oral exposure than either **1** or **9a**. The C_{max} for both **9a** and **16a** were lower than that of **1** (1,314 and 590 nM, respectively, compared to 2,587 nM for **1**).

CONCLUSION

Overall, the antiviral potency and pharmacokinetic profile of **9a** was comparable that of the prototype **1**, demonstrating that the 4-benzoic acid motif introduced at the C-3 position of BA acts as a suitable replacement for the dimethyl succinic acid side chain present in previous BA-derived MIs. This

new C-3 substituent illuminates topographical aspects of the HIV-1 MI pharmacophore by constraining the spatial relationship between the aryl carboxylic acid and the triterpenoid core and, by extension, the C-28 substituent, which can be further modified. The new analogs, in general, exhibit excellent in vitro antiviral activity against wt virus, with more modest potency changes in the presence of HSA (0.8 to 9.4-fold) than **1**, indicative of reduced serum albumin binding. However, no significant improvement in potency against Gag V370A and/or solubility were observed for the C-3 benzoic acid series when compared with **1**, with the sole exception of **9u**. Although **1** was advanced into Phase IIb clinical trials, its development was halted due to a poor antiviral responses in a significant percentage of the patient population, a liability traced to a polymorphic variations proximal to the purported binding site of the drug. In addition, high protein binding and difficulties in formulating **1** further complicated its development.²¹ A successful second generation MI will need to be able to achieve efficacy against the polymorphic viruses that show diminished antiviral susceptibility to **1**, experience a reduced effect of serum on potency and demonstrate improved physicochemical properties so as to better facilitate improved pharmacokinetic profiles. Compound **9a** exemplifies an advance toward that objective, providing a highly potent chemotype that exhibits a lower serum shift in the presence of HSA, and represents the initial effort towards finding a second generation MI.^{32,44} Further developments from this novel 4-benzoic acid deoxybetulinic acid chemotype that show enhanced activity toward polymorphic viruses, and improved physicochemical properties as the result of modification of the C-28 carboxylic acid moiety, will be reported in due course.³²

EXPERIMENTAL SECTION

Unless otherwise stated, solvents and reagents were used directly as obtained from commercial sources, and reactions were performed under a nitrogen atmosphere. Flash chromatography was conducted on

Silica gel 60 (0.040-0.063 particle size; EM Science supply). Purification was accomplished by medium pressure liquid chromatography on a Biotage flash chromatography with normal phase silica gel, or by preparative reverse phase (rp) HPLC using MeCN or MeOH-H₂O-TFA or NH₄OAc as mobile phases. Preparative rp HPLC was performed using two Shimadzu LC-8A pumps, a SPD-10AV UV-vis detector set at 220 nm and an ELSD are used. HPLC purity analyses were performed using one of the following conditions: Method A: column, Ascentis 2.7 μ m C18, 4.6 mm \times 50 mm; 90% (100% H₂O/10 mM NH₄OAc to 95% (100% MeCN). Method B: column, Supelco Acentis 2.7 μ m C18, 4.6 x 75 mm; 70% (100% H₂O/10 mM NH₄OAc) to 95% (100% MeCN/10 mM NH₄OAc); 6 min gradient; 1.5 mL/min flow rate. Method C: column, Supelco Acentis 2.7 μ m C18, 4.6 x 50 mm; 70% (100% H₂O/10 mM NH₄OAc) to 95% (100% MeCN/10 mM NH₄OAc); 5 min gradient; 2 mL/min flow rate. Method D: column, Supelco Acentis 2.7 μ m C18, 4.6 x 50 mm; 70% (100% H₂O/10 mM NH₄OAc) to 95% (100% MeCN/10 mM NH₄OAc); 6 min gradient; 2 mL/min flow rate. Method E: column, Waters Xbridge 5 μ m C18, 4.6 mm \times 50 mm; 30% (100% H₂O/10 mM NH₄OAc) to 95% (100% MeOH/10 mM NH₄OAc); 5 min gradient; 1.2 mL/min flow rate. Method F: column, Phenomenex Luna 5 μ m C5, 4.6 mm \times 150 mm; 80% (100% H₂O/10 mM NH₄OAc) to 95% (100% MeOH/10 mM NH₄OAc); 12 min gradient; 1 mL/min flow rate. Method G: column, Sunfire 5 μ m C18, 4.6 mm \times 30 mm; 95% H₂O/5% MeOH/10 mM NH₄OAc to 5% H₂O/95% MeOH/10 mM NH₄OAc; 15 min gradient; 4 mL/min flow rate. Method H: column, Sunfire 3.5 μ m C18, 4.6 mm \times 150 mm; 90% (95% H₂O/5% MeCN/0.1% TFA) to 100% (5% H₂O/95% MeCN/0.1 TFA); 15 minute gradient; 2 mL/min flow rate. Method I: column, Xbridge Phenyl 3.5 μ m, 4.6 mm \times 150 mm; 90% (95% H₂O/5% MeCN/0.1% TFA) to 100% (5% H₂O/95% MeCN/0.1 TFA); 15 minute gradient; 2 mL/min flow rate. Method J: column, Xbridge C18 3.5 μ m, 4.6 mm \times 150 mm; 90% (95% H₂O/5% MeOH/10 mM NH₄HCO₃) to 100% (5% H₂O/95% MeOH/10 mM NH₄HCO₃); 15 minute gradient; 2 mL/min flow rate. Method K: column, Xbridge Phenyl 3.5 μ m, 3.0 mm \times 150 mm; 90% (95% H₂O/5% MeCN/0.1% TFA) to 100% (5% H₂O/95%

MeCN/0.1 TFA); 15 minute gradient; 1 mL/min flow rate. Method L: column, Xbridge C18 3.5 μ m, 3.0 mm \times 150 mm; 90% (95% H₂O/5% MeOH/10 mM NH₄HCO₃) to 100% (5% H₂O/95% MeOH/10 mM NH₄HCO₃); 15 minute gradient; 1 mL/min flow rate. All Liquid Chromatography (LC) data were recorded on a Shimadzu LC-10AS liquid chromatograph using a SPD-10AV UV-Vis detector with Mass Spectrometry (MS) data determined using a Micromass Platform for LC in electrospray mode. LCMS analyses were performed using one of the following conditions: Method 1: column, Phenomenex Luna S10, 3.0 mm \times 50 mm; 95% H₂O/5% MeCN/10 mM NH₄OAc to 5% H₂O/95% MeCN/10 mM NH₄OAc; 4 min gradient; 2 mL/min flow rate. Method 2: column, Supelco Acentis 2.7 μ m C18, 4.6 x 50 mm; 70% (100% H₂O/10 mM NH₄OAc) to 95% (100% MeCN/10 mM NH₄OAc); 5 min gradient; 2 mL/min flow rate. Method 3: column, Supelco Acentis 2.7 μ m C18, 4.6 x 75 mm; 70% (100% H₂O/10 mM NH₄OAc) to 95% (100% MeCN/10 mM NH₄OAc); 6 min gradient; 1.5 mL/min flow rate. Method 4: column, Supelco Acentis 2.7 μ m C18, 4.6 x 50 mm; 70% (100% H₂O/10 mM NH₄OAc) to 95% (100% MeCN/10 mM NH₄OAc); 6 min gradient; 2 mL/min flow rate. Method 5: column, Phenomenex Luna 3 μ m C18, 3.0 mm \times 50 mm; 90% H₂O/10% MeOH/0.1% TFA to 10% water/90% MeOH/0.1% TFA; 2 min gradient; 1 mL/min flow rate. Method 6: column, Ascentis 2.7 μ m C18, 4.6 mm \times 50 mm; 90% (100% H₂O/10 mM NH₄OAc to 95% (100% MeCN); 7 min gradient; 2 mL/min flow rate. Method 7: column, Phenomenex Luna S10, 3.0 mm \times 50 mm; 95% H₂O/5% MeOH/10 mM NH₄OAc to 5% H₂O/95% MeOH/10 mM NH₄OAc; 2 min gradient; 4 mL/min flow rate. Method 8: column, Phenomenex Luna 5 μ m C5, 4.6 mm \times 150 mm; 80% (100% H₂O/10 mM NH₄OAc) to 95% (100% MeOH/10 mM NH₄OAc); 12 min gradient; 1 mL/min flow rate. Method 9: column, Waters Xbridge 5 μ m C18, 4.6 mm \times 50 mm; 30% (100% H₂O/10 mM NH₄OAc) to 95% (100% MeOH/10 mM NH₄OAc); 5 min gradient; 1.2 mL/min flow rate. Method 10: column, Phenomenex Luna 3 μ m C18, 3.0 mm \times 50 mm; 90% H₂O/10% MeCN/0.1% TFA to 10% H₂O/90% MeCN/0.1% TFA; 2 min gradient; 1 mL/min flow rate. Method 11: column, Waters Xbridge Phenyl S5, 4.6 mm \times 50 mm; 80%

(90% H₂O/10% MeOH/0.1% TFA) to 10% H₂O/90% MeOH/0.1% TFA; 1 min gradient; 4 mL/min flow rate. High-resolution mass spectra were recorded on one of the following mass spectrometers: a LCT, TOF, or a LTQ-Orbitrap instrument. ¹H NMR spectra were recorded on Bruker DRX-500f at 500 MHz (or Bruker AV 400 MHz, Bruker DPX-300B or Varian Gemini 300 at 300 MHz as stated). The chemical shifts were reported in ppm on the δ scale relative to δ TMS = 0. The following internal references were used for the residual protons in the following solvents: CDCl₃ (δ_{H} 7.26), CD₃OD (δ_{H} 3.30), Acetic-d₄ (Acetic Acid d₄) (δ_{H} 11.6, 2.07), DMSOmix or DMSO-D₆-CDCl₃ ((δ_{H} 2.50 and 8.25) (ratio 75%:25%)), and DMSO-D₆ (δ_{H} 2.50). Standard acronyms were employed to describe the multiplicity patterns: s (singlet), br. s (broad singlet), d (doublet), t (triplet), q (quartet), m (multiplet), b (broad), app (apparent). The coupling constant (J) is in Hertz.

(1R,3aS,5aR,5bR,7aR,9S,11aR,11bR,13aR,13bR)-Benzyl 9-hydroxy-5a,5b,8,8,11a-pentamethyl-1-(prop-1-en-2-yl)icosahydro-1H-cyclopenta[a]chrysene-3a-carboxylate (5). To a suspension of **3** (12 g, 26.3 mmol) and K₂CO₃ (7.26 g, 52.6 mmol) in DMF (150 mL) was added BnBr (3.28 mL, 27.6 mmol). The mixture was heated to 60 °C for 3.5 h, and cooled to rt. A solid started to precipitate upon cooling. The mixture was diluted with H₂O (200 mL) and the solid formed was collected by filtration to give **5** as a white solid (13.92 g, 97 %). ¹H NMR (500 MHz, CDCl₃) δ 7.48 - 7.27 (m, 5H), 5.26 - 5.03 (m, 2H), 4.71 (d, J = 1.83 Hz, 1H), 4.58 (s, 1H), 3.17 (dt, J = 11.4, 5.6 Hz, 1H), 3.03 (td, J = 10.99, 4.88 Hz, 1H), 2.27 (ddd, J = 12.36, 3.20, 3.05 Hz, 1H), 2.17 (td, J = 12.1, 3.5 Hz, 1H), 1.96 - 1.78 (m, 2H), 1.73 - 0.96 (m, 18H), 1.68 (s, 3H), 0.96 (s, 3H), 0.95 (s, 3H), 0.88 (td, J = 13.0, 4.1 Hz, 1H), 0.80 (s, 3H), 0.77 (s, 3H), 0.76 (s, 3H), 0.65 (d, J = 9.2 Hz, 1H).

(1R,3aS,5aR,5bR,7aR,11aR,11bR,13aR,13bR)-Benzyl 5a,5b,8,8,11a-pentamethyl-9-oxo-1-(prop-1-en-2-yl)icosahydro-1H-cyclopenta[a]chrysene-3a-carboxylate (6). To a solution of **5** (7.1 g, 12.98 mmol) in CH₂Cl₂ (100 mL) was added PCC (4.20 g, 19.48 mmol). After stirring for five minutes, the mixture turned a deep crimson color. The stirring was continued for 5.5 h. The mixture was filtered through a

pad of Celite and silica gel which was washed with CH_2Cl_2 and then a 1:1 mixture of EtOAc:hexanes. The filtrate was concentrated under reduced pressure to give **6** as a white foam (6.92 g, 98 %). ^1H NMR (500 MHz, CDCl_3) δ 7.41 - 7.28 (m, 5H), 5.20 - 5.06 (m, 2H), 4.72 (d, $J = 2.1$ Hz, 1H), 4.59 (d, $J = 1.2$ Hz, 1H), 3.01 (td, $J = 10.99, 4.88$ Hz, 1H), 2.51 - 2.43 (m, 1H), 2.42 - 2.34 (m, 1H), 2.28 (dt, $J = 12.59, 3.17$ Hz, 1H), 2.21 (td, $J = 12.28, 3.51$ Hz, 1H), 1.94 - 1.82 (m, 3H), 1.74 - 1.69 (m, 1H), 1.50 - 1.17 (m, 14H), 1.69 (s, 3H), 1.11 (dt, $J = 13.4, 2.9$ Hz, 1H), 1.07 (s, 3H), 1.03 - 0.97 (m, 1H), 1.02 (s, 3H), 0.96 (s, 3H), 0.91 (s, 3H), 0.80 (s, 3H).

(1R,3aS,5aR,5bR,7aR,11aR,11bR,13aR,13bR)-Benzyl 5a,5b,8,8,11a-pentamethyl-1-(prop-1-en-2-yl)-9-(trifluoromethylsulfonyloxy)-2,3,3a,4,5,5a,5b,6,7,7a,8,11,11a,11b,12,13,13a,13b-octadecahydro-1H-cyclopenta[a]chrysene-3a-carboxylate (7). To a solution of **6** (6.9 g, 12.67 mmol) and 1,1,1-trifluoro-*N*-phenyl-*N*-(trifluoromethylsulfonyl)methanesulfonamide (9.05 g, 25.3 mmol) in THF (200 mL) at -78°C was added KHMDS (50.7 mL, 25.3 mmol) slowly. The reaction mixture was stirred for 1 h at -78°C . TLC indicated starting material was consumed and desired product was formed. The reaction mixture was quenched with brine (100 mL) and extracted with Et_2O (3 x 100 mL). The extracts were dried over Na_2SO_4 , filtered and concentrated under reduced pressure. The residue was dissolved in toluene and purified by flash chromatography using 2-10% toluene/hexanes and 5-10% ethyl EtOAc/hexanes to provide the desired product **7** as a white solid (7.36 g, 86%). ^1H NMR (500 MHz, CDCl_3) δ 7.45 - 7.32 (m, 5H), 5.56 (dd, $J = 6.71, 1.53$ Hz, 1H), 5.22 - 5.06 (m, 1H), 5.12 - 5.05 (m, 1H), 4.74 (d, $J = 2.14$ Hz, 1H), 4.61 (dd, $J = 1.37, 2.29$ Hz, 1H), 3.04 (td, $J = 10.99, 4.58$ Hz, 1H), 2.31 (dt, $J = 12.7, 3.2$ Hz, 1H), 2.22 (td, $J = 12.21, 3.36$ Hz, 1H), 2.17 (dd, $J = 17.09, 6.71$ Hz, 1H), 2.00 - 1.81 (m, 2H), 1.80 - 1.72 (m, 2H), 1.69 (s, 3H), 1.52 - 1.25 (m, 12H), 1.25 - 1.19 (m, 1H), 1.16 (t, $J = 3.1$ Hz, 1H), 1.12 (s, 3H), 1.01 (s, 3H), 1.08 - 1.03 (m, 1H), 0.96 (s, 3H), 0.89 (s, 3H), 0.79 (s, 3H). ^{13}C NMR (127 MHz, CDCl_3) δ : 175.5, 155.1, 150.2, 136.2, 128.2, 128.0, 127.8, 113.5, 109.4, 65.5, 56.3, 53.0, 49.1, 48.7, 46.7, 42.1,

40.3, 40.0, 38.0, 37.6, 36.6, 36.0, 33.0, 31.8, 30.3, 29.3, 27.2, 25.3, 21.2, 19.2, 19.1, 18.7, 15.9, 15.2, 14.4.

General method for the preparation of compounds 9a-9i, 9k-9q and 9s-9u.

Step 1: Suzuki coupling. To a sealable vial containing **7** (1.0 equiv.) was added the corresponding boronic acid (1.1-1.5 equiv.), Na₂CO₃ (5 equiv.) and Pd(PPh₃)₄ (0.03-0.1 equiv.). The mixture was diluted with either a mixture of DME:water (1:0.5-1.0), or a mixture of 1,4-dioxane:water (1:0.5-1.0) to a concentration of 0.015 M-0.074 M. The vial was flushed with N₂, sealed, and heated to 85 °C-100 °C. After 1.5 -24 h of heating, the mixture was cooled to rt. The mixture was diluted with either sat. NH₄Cl, 1N HCl, or water and extracted with CH₂Cl₂ or EtOAc. The combined organic layers were dried with sodium sulfate. The drying agent was removed by filtration and the filtrate was concentrated under reduced pressure. The residue was either used directly in the next step, or was purified by flash chromatography to afford the expected cross-coupling product which was used in the next step.

Step 2: Deprotection of carboxylic acid (9a-9i, 9k-9q and 9s-9u). A mixture of the corresponding Suzuki coupling product from the previous step (1.0 equiv.) and 10% Pd/C (0.1-1 equiv.) in either EtOAc or a mixture of EtOAc: MeOH (1:0.5-1.0) to a concentration of 0.01M - 0.06 M was stirred under 1 atm of H₂ for 1-24 h. The reaction mixture was filtered and the white solid formed was collected. The solids were purified by prep. HPLC to provide the desired products **9a-9i, 9k-9q and 9s-9u** as white solids.

(1R,3aS,5aR,5bR,7aR,11aS,13aR,13bR)-9-(4-Carboxyphenyl)-5a,5b,8,8,11a-pentamethyl-1-(prop-1-en-2-yl)-2,3,3a,4,5,5a,5b,6,7,7a,8,11,11a,11b,12,13,13a,13b-octadecahydro-1H-cyclopenta[a]chrysene-3a-carboxylic acid (9a). The title compound **9a** was prepared following general method for the preparation of compounds **9a-9i, 9k-9q and 9s-9u** described above using 4-boronobenzoic acid as the reactant boronic acid. The product was isolated as a white solid (10 mg,

40%). The compound was purified by preparative HPLC with 20-100 90% MeCN/10% H₂O/0.1% TFA was then washed with saturated NaHCO₃ followed by 1 N HCl and submitted for Elemental Analysis. LCMS: m/e 557.46 (M-H)⁻, 5.44 min (method 6). ¹H NMR (500 MHz, DMSO-D₆) δ 7.73 (d, *J* = 7.93 Hz, 2H), 6.96 (d, *J* = 7.63 Hz, 2H), 5.18 (d, *J* = 5.80 Hz, 1H), 4.69 (s, 1H), 4.56 (s, 1H), 3.07 - 2.92 (m, 1H), 2.50 - 2.43 (m, 1H), 2.38 - 2.31 (m, 1H), 2.13 (d, *J* = 12.51 Hz, 1H), 2.04 (dd, *J* = 6.41, 17.09 Hz, 1H), 1.89 - 1.75 (m, 2H), 1.68-1.62 (m, 2H), 1.58-1.08 (m, 13H), 1.04 - 0.98 (m, 1H), 1.66 (s, 3H), 0.97 (s, 3 H), 0.96 (s, 6H), 0.88 (s, 3 H), 0.86 (s, 3H). ¹³C NMR (101MHz, DMSO-D₆) δ 177.4, 167.4, 150.5, 147.9, 146.0, 130.0, 128.8, 128.5, 123.8, 109.7, 55.7, 52.4, 48.9, 48.7, 46.7, 42.2, 41.2, 40.2, 37.9, 37.1, 36.5, 35.9, 33.3, 31.8, 30.3, 29.4, 25.3, 21.1, 19.4, 19.2, 16.4, 15.6, 14.5. Anal. Calcd for C₃₇H₅₃ClO₅: C, 72.46; H, 8.71; N, 0. Found: C, 72.51; H, 8.68; N, <0.02. HRMS for C₃₇H₄₉O₄, (M - H)⁻ calcd 557.3625, found 557.3629. Anal. rp-HPLC: *t*_R = 5.44 min (method A, purity = 100 %).

(1*R*,3*aS*,5*aR*,5*bR*,7*aR*,11*aS*,11*bR*,13*aR*,13*bR*)-Benzyl 5*a*,5*b*,8,8,11*a*-pentamethyl-1-(prop-1-en-2-yl)-9-(1*H*-pyrazol-5-yl)-2,3,3*a*,4,5,5*a*,5*b*,6,7,7*a*,8,11,11*a*,11*b*,12,13,13*a*,13*b*-octadecahydro-1*H*-cyclopenta[*a*]chrysene-3*a*-carboxylate (10). To flask containing **7** (250 mg, 0.369 mmol) was added 1*H*-pyrazole-5-boronic acid (49.6 mg, 0.443 mmol), Na₂CO₃·H₂O (137.0 mg, 1.11 mmol) and Pd(PPh₃)₄ (12.8 mg, 0.011 mmol). The mixture was diluted with 1,4-dioxane (4.0 mL) and H₂O (1.0 mL), then was flushed with N₂ and was heated to 85 °C for 5.5 h. The mixture was cooled to rt and stirred overnight. The mixture was diluted with H₂O (15 mL) and extracted with EtOAc (3 x 15 mL). The combined organic layers were washed with brine, dried over MgSO₄, filtered and concentrated under reduced pressure. The residue was purified by flash chromatography using a 0-20% EtOAc/hexanes with 0.1% NH₄OH added to the mobile phase. The fractions containing the product were combined and concentrated under reduced pressure to give **10** as a white foam (134.0 mg, 61%). LCMS: m/e 595.2 (M+H)⁺, 2.60 min (method 10). ¹H NMR (500MHz, CDCl₃) δ 7.50 (d, *J* = 1.8 Hz, 1H), 7.40 - 7.29 (m, 5H), 6.20 (d, *J* = 1.8 Hz, 1H), 5.74 - 5.70 (m, 1H), 5.17 (d, *J* = 12.5 Hz, 1H), 5.10 (d, *J* = 12.5 Hz, 1H),

4.74 (d, $J = 1.5$ Hz, 1H), 4.61 (s, 1H), 3.04 (td, $J = 10.8, 4.6$ Hz, 1H), 2.32 - 2.19 (m, 2H), 2.14 (dd, $J = 17.5, 6.6$ Hz, 1H), 1.95 - 1.81 (m, 2H), 1.76 - 0.86 (m, 17H), 1.70 (s, 3H), 1.06 (s, 3H), 1.04 (s, 3H), 0.98 (s, 3H), 0.91 (s, 3H), 0.82 (s, 3H).

(1R,3aS,5aR,5bR,7aR,11aS,11bR,13aR,13bR)-Benzyl 9-(1-(2-ethoxy-2-oxoethyl)-1H-pyrazol-3-yl)-5a,5b,8,8,11a-pentamethyl-1-(prop-1-en-2-yl)-2,3,3a,4,5,5a,5b,6,7,7a,8,11,11a,11b,12,13,13a,13b-octadecahydro-1H-cyclopenta[a]chrysene-3a-carboxylate (11). To a solution of **10** (130 mg, 0.219 mmol) in DMF (2 mL) was added K_2CO_3 (91 mg, 0.656 mmol) followed by ethyl bromoacetate (0.121 mL, 1.093 mmol). The mixture was heated to 75 °C for 17 h then cooled to rt, diluted with H_2O (30 mL) and extracted with CH_2Cl_2 (3 x 30 mL). The combined organic layers were dried over Na_2SO_4 , filtered and concentrated under reduced pressure. The crude product was combined with the crude product from a smaller test experiment (0.096 mmol scale) and was purified by flash chromatography using a 0-15% EtOAc/hexanes with 0.1% NH_4OH to the mobile phase on a 25 g silica gel column. The fractions containing the product were combined and concentrated under reduced pressure. TLC showed separation was not complete, and the product contained an impurity. The product was purified a second time by flash chromatography using a 0-10% EtOAc/hexanes with 0-1% NH_4OH added to the mixture. The fractions containing the expected product were combined and concentrated under reduced pressure to give **11** as a clear film (0.157g, 73%). LCMS: m/e 681.6 ($M+H$)⁺, 4.01 min (method 5). 1H NMR (500MHz, $CDCl_3$) δ 7.40 - 7.28 (m, 6H), 6.22 (d, $J = 2.4$ Hz, 1H), 5.79 (dd, $J = 6.4, 1.8$ Hz, 1H), 5.17 (d, $J = 12.2$ Hz, 1H), 5.10 (d, $J = 11.6$ Hz, 1H), 4.87 (s, 2H), 4.74 (d, $J = 2.1$ Hz, 1H), 4.6 (s, 1H), 4.21 (q, $J = 7.1$ Hz, 2H), 3.05 (td, $J = 10.9, 4.7$ Hz, 1H), 2.30 - 2.25 (m, 1H), 2.25 - 2.18 (m, 1H), 2.11 (dd, $J = 17.4, 6.4$ Hz, 1H), 1.94 - 1.82 (m, 2H), 1.74 - 0.86 (m, 17H), 1.69 (s, 3H), 1.26 (t, $J = 6.7$ Hz, 3H), 1.12 (s, 3H), 1.09 (s, 3H), 0.97 (s, 3H), 0.92 (s, 3H), 0.82 (s, 3H).

(1R,3aS,5aR,5bR,7aR,11aS,11bR,13aR,13bR)-9-(1-(2-Ethoxy-2-oxoethyl)-1H-pyrazol-3-yl)-5a,5b,8,8,11a-pentamethyl-1-(prop-1-en-2-yl)-2,3,3a,4,5,5a,5b,6,7,7a,8,11,11a,11b,12,13,13a,13b-

octadecahydro-1H-cyclopenta[a]chrysene-3a-carboxylic acid (12). To a solution of **11** (0.157 g, 0.231 mmol) in DCE (3 mL) was added TEA (0.051 mL, 0.369 mmol), *t*-butyldimethylsilane (0.076 mL, 0.461 mmol) and Pd(OAc)₂ (0.013 g, 0.058 mmol). The mixture was flushed with N₂ and heated to 60 °C for 4h. An additional 76 µL of *t*-butyldimethylsilane was added to the mixture along with 13 mg of Pd(OAc)₂. The mixture was flushed with N₂ and heated to 60 °C for an additional 3.5 hours. The mixture was cooled to rt, and stirred for three days, dissolved in DCM, filtered through a pad of Celite and concentrated under reduced pressure. The residue was purified by flash chromatography using a 0-25% EtOAc/hexanes to provide **12** as a clear film (0.075g, 55%). LCMS: m/e 591.6 (M+H)⁺, 2.53 min (method 10). ¹H NMR (400 MHz, CDCl₃) δ 7.36 (d, *J* = 2.26 Hz, 1H), 6.23 (d, *J* = 2.51 Hz, 1H), 5.80 (dd, *J* = 1.76, 6.27 Hz, 1H), 4.89 (s, 2H), 4.76 (d, *J* = 1.51 Hz, 1H), 4.63 (s, 1H), 4.22 (q, *J* = 7.28 Hz, 2H), 3.04 (dt, *J* = 4.39, 10.73 Hz, 1H), 2.33 - 2.22 (m, 2H), 2.15 (dd, *J* = 6.40, 17.44 Hz, 1H), 2.07 - 1.95 (m, 2H), 1.78 - 0.97 (m, 17H), 0.97 (m, 17H), 1.71 (s, 3H), 1.27 (t, *J* = 7.15 Hz, 3H), 1.12 (s, 3H), 1.10 (s, 3H), 1.00 (s, 3H), 1.00 (s, 3H), 0.95 (s, 3H).

(1R,3aS,5aR,5bR,7aR,11aS,11bR,13aR,13bR)-9-(1-(Carboxymethyl)-1H-pyrazol-3-yl)-5a,5b,8,8,11a-pentamethyl-1-(prop-1-en-2-yl)-2,3,3a,4,5,5a,5b,6,7,7a,8,11,11a,11b,12,13,13a,13b-octadecahydro-1H-cyclopenta[a]chrysene-3a-carboxylic acid (9r). To a solution of **12** (74 mg, 0.125 mmol) in 1,4-dioxane (2 mL) was added NaOH (1N) (0.5 mL, 0.500 mmol). The mixture was heated to 85 °C for 17.5 h then cooled to rt, diluted with MeOH and purified by prep HPLC. The fractions containing the expected product were combined and concentrated under reduced pressure to give **9r** as a white solid (54 mg, 77 %). LCMS: m/e 563.5 (M+H)⁺, 2.26 min (method 10). ¹H NMR (500 MHz, acetic acid-d₄) δ 7.54 (d, *J* = 2.14 Hz, 1H), 6.24 (d, *J* = 2.44 Hz, 1H), 5.69 (dd, *J* = 1.68, 6.26 Hz, 1H), 5.13 (s, 2H), 4.77 (d, *J* = 1.53 Hz, 1H), 4.63 (s, 1H), 3.05 (dt, *J* = 4.73, 10.76 Hz, 1H), 2.38 - 2.26 (m, 2H), 2.21 - 1.00 (m, 20H), 1.72 (s, 3H), 1.06 (s, 6H), 1.03 (s, 3H), 1.02 (s, 3H), 0.98 (s, 3H). HRMS for

$C_{35}H_{49}O_4N_2$, (M - H)⁻ calcd 561.3687, found 561.3710. Anal. rp-HPLC: t_R = 10.22 min (method I, purity = 100 %).

((1R,3aS,5aR,5bR,7aR,9S,11aR,11bR,13aR,13bR)-9-Hydroxy-5a,5b,8,8,11a-pentamethyl-1-(prop-1-en-2-yl)icosahydro-1H-cyclopenta[a]chrysen-3a-yl)methyl benzoate (13). A mixture of **4** (2.5 g, 5.65 mmol), benzoic anhydride (2.147 mL, 11.29 mmol) and DMAP (0.690 g, 5.65 mmol) was heated in pyridine (50 mL) at 60°C for 3h. The mixture was cooled to rt then was quenched with H₂O and concentrated under reduced pressure to remove most of the pyridine. CH₂Cl₂ was added to the residue and the organic phase was separated and dried over Na₂SO₄. The drying agent was removed by filtration and the filtrate was concentrated under reduced pressure. The crude material containing **13** was taken to the next step without further purification.

((1R,3aS,5aR,5bR,7aR,11aR,11bR,13aR,13bR)-5a,5b,8,8,11a-Pentamethyl-9-oxo-1-(prop-1-en-2-yl)icosahydro-1H-cyclopenta[a]chrysen-3a-yl)methyl benzoate (14). The crude material containing compound **13** (2.98 g, 5.45 mmol) from above was dissolved in CH₂Cl₂ (50 mL) and treated with PCC (1.762 g, 8.18 mmol). The mixture was stirred at rt for 2 h. TLC showed no starting material and one less polar product. The mixture was filtered through Celite and silica gel and the filtrate was concentrated under reduced pressure to afford the desire product **14** as a white solid which was used in the next step without further purification. LCMS: m/e 545.45 (M+H)⁺, 2.71 min (method 11).

((1R,3aS,5aR,5bR,7aR,11aR,11bR,13aR,13bR)-5a,5b,8,8,11a-Pentamethyl-1-(prop-1-en-2-yl)-9-(trifluoromethylsulfonyloxy)-2,3,3a,4,5,5a,5b,6,7,7a,8,11,11a,11b,12,13,13a,13b-octadecahydro-1H-cyclopenta[a]chrysen-3a-yl)methyl benzoate (15). A mixture of **14** (3.89 g, 10.90 mmol) and *N*-phenylbis(trifluoromethane)sulfonimide (3.89 g, 10.90 mmol) was stirred in THF (30 mL) at -78°C. KHMDS (0.5 in toluene) (21.80 mL, 10.90 mmol) was slowly added and the reaction mixture was kept at -78°C for 1 h. TLC showed starting material and a less polar spot. KHMDS (1eq, 5 ml) was added and the mixture was stirred at -78°C for 1 h longer. The reaction mixture was quenched with brine and

warmed at rt. The organic layer was extracted with Et₂O and dried over Na₂SO₄, filtered, concentrated and purified using silica gel (0-10% toluene/hexanes) to provide the desired product **15** as a white solid (2.22 g, 60.2 % yield over 3 steps). ¹H NMR (400 MHz, CDCl₃) δ 8.09 - 8.05 (m, 2H). 7.60 - 7.55 (m, 1H), 7.49 - 7.43 (m, 2H), 5.58 (dd, *J* = 6.65, 1.88 Hz, 1H), 4.75 (d, *J* = 2.01 Hz, 1H), 4.64 (s, 1H), 4.55 (dd, *J* = 11.04, 1.25 Hz, 1H), 4.12 (d, *J* = 11.04 Hz, 1H), 2.56 (td, *J* = 11.11, 5.90 Hz, 1H), 2.18 (dd, *J* = 17.07, 6.78 Hz, 1H), 2.13 - 1.92 (m, 3H), 1.86 - 1.10 (m, 18H), 1.73 (s, 3H), 1.14 (s, 3H), 1.11 (s, 3H), 1.03 (s, 3H), 1.03 (s, 3H), 0.94 (s, 3H).

General method for the preparation of compounds **16a-16q**.

Step 1: Suzuki coupling. To a sealable vial containing **15** (0.074 -0.322 mmol) was added the corresponding boronic acid (1.05-1.5 equiv.), base (either K₃PO₄ (4 equiv.), K₂CO₃ (3 equiv.-10 equiv.) or Na₂CO₃·H₂O (3 equiv.-10 equiv.)), and Pd(PPh₃)₄ (0.03-0.2 equiv.). The mixture was diluted with either 1,4-dioxane, DME, a mixture of 1,4-dioxane:H₂O (1-4:1), a mixture of DME:H₂O (1-4:1), a mixture of 2-propanol: H₂O (4:1), or a mixture of 1,4-dioxane:2-propanol: H₂O (2:2:1) to a concentration of 0.059-0.074 M. The vial was flushed with N₂, sealed, and heated to 85°C-100°C. After 3-24 h of heating, the mixture was cooled to rt. The mixture was diluted with either saturated NH₄Cl, 1N HCl, or H₂O and extracted with CH₂Cl₂. The combined organic layers were dried over Na₂SO₄. The drying agent was removed by filtration and the filtrate was concentrated under reduced pressure. The residue was either used directly in the next step, or was purified by flash chromatography to afford the expected cross-coupling product which was used in the next step.

Stille coupling: To a sealable vial containing **15** (0.111 mmol) was added the corresponding tributylstannyl reagents (1.35 equiv.), lithium chloride (3 equiv.), and Pd(PPh₃)₄ (0.05 equiv.). The mixture was diluted with 1,4-dioxane (2 mL) and flushed with N₂. The vial was sealed and heated to 85 °C for 15.5 h. The mixture was cooled to rt, diluted with water (4 mL) and extracted with CH₂Cl₂ (3 x 4

mL). The combined organic layers were dried over Na₂SO₄. The drying agent was removed by filtration and the filtrate was concentrated under reduced pressure. The residue purified by flash chromatography using a 0-25% EtOAc/hexanes to afford the expected C-3 cross-coupling product which was used in the next step.

Step 2: Deprotection of alcohol (16a-16q): To a solution of the C-3 cross-coupling products from the previous step (0.058 - 0.295 mmol) in dioxane:water (1:1, 3:1 or 4:1) was added LiOH·H₂O (19-43 equiv.) or 1N NaOH (10 equiv.) The mixture was heated to 75 °C for 3-18 h, was cooled to rt, and was quenched with 1N HCl. The mixture was extracted with CH₂Cl₂ or EtOAc and the organic layers were combined and dried over Na₂SO₄. The drying agent was removed by filtration and the filtrate concentrated under reduced pressure. The residue was purified by either flash chromatography, crystallization from dioxane and H₂O, or prep HPLC to give the expected deprotected product **16a-16q**.

4-((1R,3aS,5aR,5bR,7aR,11aS,11bR,13bR)-3a-(Hydroxymethyl)-5a,5b,8,8,11a-pentamethyl-1-(prop-1-en-2-yl)-2,3,3a,4,5,5a,5b,6,7,7a,8,11,11a,11b,12,13,13a,13b-octadecahydro-1H-cyclopenta[a]chrysen-9-yl)benzoic acid (16a). The title compound **16a** was prepared following the general method for the preparation of compounds **16a-16q** described above using 4-ethoxycarbonylphenylboronic acid as the reactant boronic acid. The product was purified by flash chromatography using a 0-5% MeOH in CH₂Cl₂ gradient followed by crystallization from dioxane and H₂O. The product was isolated as a white solid (12 mg, 30% yield over two steps). LCMS: m/e 543.6 (M-H)⁺, 1.82 min (method 1). ¹H NMR (400 MHz, Pyr-D₅) δ 8.47 (d, *J* = 8.03 Hz, 2H), 7.42 (d, *J* = 8.03 Hz, 2H), 5.42 (d, *J* = 4.52 Hz, 1H), 4.94 (d, *J* = 2.26 Hz, 1H), 4.80 (s, 1H), 4.14 (d, *J* = 10.79 Hz, 1H), 3.71 (d, *J* = 10.79 Hz, 1H), 2.68 (td, *J* = 10.92, 5.77 Hz, 1H), 2.52 - 2.41 (m, 2H), 2.27 - 2.09 (m, 2H), 2.02 - 1.11 (m, 18H), 1.82 (s, 3H), 1.10 (s, 6H), 1.03 (s, 6H), 1.02 (s, 3H). ¹³C NMR (126MHz, DMSO-D₆) δ 167.2, 150.4, 147.6, 145.8, 129.7, 128.9, 128.3, 123.6, 109.6, 57.9, 52.2, 48.7, 48.1, 47.4, 47.3, 42.2, 41.0, 40.3, 36.9, 36.9, 35.7, 33.8, 33.0, 29.3, 29.2, 29.0, 26.6, 24.9, 20.9, 20.8, 19.3, 18.8,

16.2, 15.3, 14.4. Anal. Calcd for $C_{37}H_{52}O_3$: C, 81.57; H, 9.62; N, 0. Found: C, 81.24; H, 9.63; N, <0.02. HRMS for $C_{37}H_{53}O_3$, $(M + H)^+$ calcd 545.3989, found 545.3972. Anal. rp-HPLC: t_R = 17.19 min (method J, purity = 100 %).

HIV cell culture assay:

Cells. MT-2 cells were obtained from the NIH AIDS Research and Reference Reagent Program and sub-cultured twice a week in RPMI 1640 media supplemented with 10% heat inactivated fetal bovine serum (FBS), 100 units/mL of penicillin G and 100 units/mL of streptomycin. The DMEM medium was additionally supplemented with 10 mM HEPES buffer, pH 7.55, 2 mM L-glutamine and 0.25 μ g/mL of amphotericin B.

Viruses. NLRepRluc virus contains the *Renilla* luciferase marker in place of the viral *nef* gene. The proviral plasmid pNLRepRluc was constructed at Bristol-Myers Squibb starting from a proviral NL₄₋₃ clone (B subtype) that was obtained from the NIH AIDS Research and Reference Reagent Program. The parent recombinant wt virus (NLRepRlucP373S) was derived from pNLRepRluc and contained the additional substitution of P373 for serine in the Gag gene (within the SP1 spacer). A serine at position 373 is the most common variation at that position among in subtype B viruses. The other recombinant viruses were generated by site-directed mutagenesis of plasmid pNLRepRlucP373S to introduce amino acid substitutions representing important polymorphic variations in Gag. The recombinant virus DNA was then used to generate virus stocks by transfecting HEK293T cells (Lipofectamine PLUS kit, Invitrogen).

Titers of virus stocks were determined using as a virus infectivity assay⁴⁵ with a luciferase endpoint (Dual-Luciferase® Reporter Assay System, Promega, Milwaukee, WI, USA) as endpoints. The TCID₅₀/mL (50% tissue culture infectious dose) was calculated by the method of Spearman-Kärber.

Multiple cycle drug susceptibility assays. Pellets of MT-2 cells were infected with either the NLRepRlucP373S wild type virus or one with a V370A site-directed mutation in the *gag* gene that has been reported to reduce susceptibility to BVM¹⁸. Initial *inocula* of the reporter strains in these assays were normalized using equivalent endpoint luciferase activity signals. Cell-virus mixtures were re-suspended in medium, incubated for 1-hour at 37°C/CO₂, and added to compound containing 96-well plates at a final cell density of 50,000 cells per ml, a concentration found to permit exponential cell growth (total volume 200 μ L). The test compounds were 3-fold serially diluted in 100% DMSO, and

assayed at a final DMSO concentration of 1%. After 4-5 day incubation at 37°C/CO₂, virus yields were determined by *Renilla* luciferase activity (Dual-Luciferase® Reporter Assay System, Promega).

Serum effects in multiple cycle drug susceptibility assay were determined by supplementing the 10 % FBS medium with 15 mg/mL of HSA. The serum effect was calculated as the change in EC₅₀ in the presence of HSA versus the EC₅₀ in the absence of HSA.

The 50% inhibitory concentrations (EC₅₀) were calculated by using the exponential form of the median effect equation where Percent Inhibition = 100 x (1/(1 + (EC₅₀/drug conc.)^m)), where m is a parameter that reflects the slope of the concentration-response curve. Background was taken as the residual signal observed upon inhibition at the highest concentration of a control protease inhibitor, NFV (3 µM).

In vitro Gag p25 cleavage assays. **1** and **9a** were evaluated for their ability to inhibit p25 cleavage by transfection of pGagOpt into 293T cells (encodes full length HIV-1 LAI Gag, producing HIV-1 VLPs). VLPs were harvested by centrifugation of supernatants at 14K and VLPs were subsequently cleaved *ex vivo* by purified HIV-1 protease in the absence or presence of the specified concentration of inhibitor. HIV-1 Gag cleavage products were analyzed by Western analysis using a primary anti-p24 monoclonal antibody (Perkin Elmer, NEA9306001) and a secondary goat anti-mouse antibody (Biorad, RPN2132, Hercules, California, USA), and then developed with the ECL Plus detection kit (Amersham, Marlborough, MA, USA). Intensities of p25 (25 kDa) and p24 (24 kDa) total cleavage products in each lane were quantified using a STORM 860 phosphorimager (Molecular Dynamics, Sunnyvale, CA, USA) and expressed as ratios of p25/p24.

Kinetics of MI dissociation from HIV-1 Gag VLPs. MI dissociation rates were measured by adding 30 nM [³H]-dihydro **1**⁴³ to SPA bead/HIV-1 VLP (0.5 to 1.2 µg) complexes, allowing binding to reach equilibrium for 3 hours at room temperature. After this time, a 40-fold molar excess of unlabeled competitor MI (**9a**) was added to effect irreversible displacement of the [³H] MI. Kinetics of disappearance of the bond [³H] MI were monitored using a Microbeta2 plate reader (PerkinElmer) and the data fitted to a first order exponential equation (GraphPad Prism v5.1).

Evaluation of in vitro metabolism rates in liver microsomes:

Compound (0.5 µM) was incubated with liver microsomes (1 mg/mL) in the presence of NADPH (1.0 mM) and MgCl₂ (5 mM). Metabolic reaction was terminated (quenched) with MeOH and MeCN (1:3 v/v) containing an internal standard at multiple time points. Metabolism rate was determined based on the parent compound disappearance over time, as measured by LC-MS/MS.

In vivo studies:

All animal studies were performed under the approval of the Bristol-Myers Squibb Animal Care and Use Committee and in accordance with the American Association for Accreditation of Laboratory Animal Care. Animals were dosed IV by cannula implanted in an acceptable vein with an infusion period of 10 min. Vehicle was 89% PEG-300, 10% ethanol and 1% TWEEN 80. Animals were dosed orally by gavage following an overnight fast. Oral solution vehicle was the same as IV dosing. Blood was collected via a venous port and centrifuged to obtain plasma. Samples were treated with MeCN containing an internal standard, centrifuged and analyzed by LC-MS/MS. Pharmacokinetic parameters were obtained by non-compartmental analysis of plasma concentration versus time data (KINETICA™ software).

AUTHOR INFORMATION

Corresponding Authors:

*For Z. L.: phone, +1 203 677 6057; fax, +1 203 677 7884; E-mail, Zheng.Liu@bms.com.

*For A. R-R., phone, +1 203 677 7416; fax, +1 203 677 7884; E-mail, Alicia.regueiroren@bms.com.

ACKNOWLEDGMENTS

We thank John E. Leet and Katalin Ebinger for compound purification, Yan He for help with structure elucidation, Brett R. Beno for evaluating the overlay of compounds and Tatyana Zvyaga for metabolic stability data.

ABBREVIATIONS USED

AUC: area under the curve; BA: betulinic acid; BVM: bevirimat; CA: capsid; calcd: calculated; cART, combination antiretroviral therapy; CL: clearance; C_{\max} : the maximum concentration of a drug in the

body after dosing; CMP: counts per minute; CV: confidence value; DCM: methylene chloride; DMAP: dimethylaminopyridine; DME: 1,2-dimethoxyethane; DMF: dimethylformamide; DMSOmix or DMSO- D_6 - $CDCl_3$: dimethyl sulfoxide- d_6 mix or dimethyl sulfoxide- d_6 -chloroform- d ; EA: elemental analysis; ELSD: evaporative light scattering detector; EtOAc: ethyl acetate; F: oral bioavailability; FBS: fetal bovine serum; FC: fold change; HPLC: high performance liquid chromatography; HSA: human serum albumin; IV: intravenous; LC: liquid chromatography; KHMDs: potassium bis (trimethylsilyl)amide; MA: matrix; MI: maturation inhibitor; MeOH: methanol; MOA: mechanism of action; MS: mass spectrometry; NADPH: dihydronicotinamide-adenine dinucleotide phosphate; NC: nucleocapsid; NFV: nelfinavir; PCC: pyridinium chlorochromate; $Pd(Ph_3P)_4$: tetrakis(triphenylphosphine)palladium(0); PEG: polyethyleneglycol; PK: pharmacokinetic; PO: *per os*, oral; RP: reverse phase; SD: standard deviation; SP: spacer peptide; TFA: trifluoroacetic acid; THF: tetrahydrofuran; TLC: thin layer chromatography; VLP: viral-like particle; Vss: volume of distribution; wt: wild-type.

SUPPLEMENTARY INFORMATION

Figure S1 with complete the complete Western blot (abstracted for p25/p24 in Figure 3) and methods of preparation and characterization for compounds **9b-9q**, **9s-9u** and **16b-16q** are available in the SI section.

REFERENCES

- (1) Taiwo, B.; Hicks, C.; Eron, J. Unmet therapeutic needs in the new era of combination antiretroviral therapy for HIV-1. *J. Antimicrob. Chemother.* **2010**, *65*, 1100-1107.
- (2) Mehellou, Y.; De Clercq, E. Twenty-six years of anti-HIV drug discovery: where do we stand and where do we go? *J. Med. Chem.* **2010**, *53*, 521-538.
- (3) Pau, A. K.; George, J. M. Antiretroviral therapy. *Infect. Dis. Clin. N. Am.* **2014**, *28*, 371-402.

- (4) Pau, B.; Holodniy, M. Novel targets for antiretroviral therapy: clinical progress to date. *Drugs* **2009**, *69*, 31–50.
- (5) Paterson D. L.; Swindells, S.; Mohr, J.; Brester, M.; Vergis, E. N.; Squier, C.; Wagener, M. M.; Singh, N. Adherence to protease inhibitor therapy and outcomes in patients with HIV infection. *Ann. Intern. Med.* **2000**, *133*, 21–30.
- (6) Wainberg, M. A.; Zaharatos, G. J.; Brenner, B. G. Development of antiretroviral drug resistance. *N. Engl. J. Med.* **2011**, *365*, 637–646.
- (7) Yu, D.; Wild, C. T.; Martin, D. E.; Morris-Natschke, S. L.; Chen, C. H.; Allaway, G. P.; Lee, K. H. The discovery of a class of novel HIV-1 maturation inhibitors and their potential in the therapy of HIV. *Expert Opin. Investig. Drugs* **2005**, *14*, 681.
- (8) (a) Gerrish, D.; Kim, I. C.; Kumar, D. V.; Austin, H.; Garrus, J. E.; Baichwal, V.; Saders, M.; McKinnon, R. S.; Anderson, M. B.; Carlson, R.; Arranz-Plaza, E.; Yager, K. M. Triterpene based compounds with potent anti-maturation activity against HIV-1. *Bioorg. Med. Chem. Lett.* **2008**, *18*, 6377–6380. Kumar, D. V. (b) Kumar, D. V.; Gerrish, D.; Hoarau, C.; Yager, K.; Austin, H.; McKinnon, R.; Dorweiler, I.; Brown, B.; Baichwal, V.; Papac, D.; Bradford, C.; Patton, S.; Bulka, K.; De Mie, L.; Carlson, R. Next generation orally bio-available HIV maturation inhibitors. Abstracts of Papers, *239th ACS National Meeting and Exposition*, San Francisco, CA, United States, March 21–25, 2010, MEDI-137.
- (9) Blair, W. S.; Cao J.; Fok-Seang J.; Griffin P.; Isaacson J.; Jackson R L.; Murray E.; Patick, A. K.; Peng Q.; Perros M.; Pickford C.; Wu H.; Butler S. L. New small-molecule inhibitor class targeting human immunodeficiency virus type 1 virion maturation. *Antimicrob. Agents Chemother.* **2009**, *53*, 5080–5087.

- (10) Coric, P.; Turcaud, S.; Souquet, F.; Briant, L.; Gay, B.; Royer, J.; Chazal, N.; Bouaziz, S. Synthesis and biological evaluation of a new derivative of bevirimat that targets the Gag CA-SP1 cleavage site. *Eur. J. Med. Chem.* **2013**, *62*, 453-465.
- (11) (a) Urano, E.; Ablan, S. D.; Martin, D.; Gaur, R.; Keller, P. W.; Steven, A. C.; Nitz, T.; Wild, C.; Freed, E. O. Recent progress in the development of potent and broadly active HIV-1 Maturation Inhibitors. *21st Conference on Retroviruses and Opportunistic Infections*, Boston, MA. March 3-6, **2014**. Abstract # 536. (b) Jeffrey, J. L.; Wang, P.; McDanal, C.; Schipper, P. J.; Brown, K.; Galardi, C.; Tang, J.; Nijhuis, M.; Johns, B. A. GSK2838232, a second generation HIV-1 maturation inhibitor with an optimized virology profile. *22nd Conference on Retroviruses and Opportunistic Infections*, Seattle, WA. February 23-26, **2015**; O-10. Abstract #538.
- (12) (a) Lingappa, J. R.; Jonathan C. Reed, J. C.; Tanaka, M.; Chutiraka, K.; Robinson, B. A. How HIV-1 Gag assembles in cells: putting together pieces of the puzzle. *Virus Res.* **2014**, *193*, 98-107. (b) Neil M. Bell, N. M.; Lever, A. M. L. HIV Gag polyprotein: processing and early viral particle assembly. *Trends Microbiol.* **2013**, *21*, 136-144. (c) Lee, S. K.; Potempa M.; Swanstrom, R. The choreography of HIV-1 proteolytic processing and virion assembly. *J. Biol. Chem.* **2012**, *287*, 40867-40874. (d) Sundquist, W. I.; Kräusslich, H. G. HIV-1 assembly, budding, and maturation. *Cold Spring Harb. Perspect. Med.* **2012**, (7):a006924.
- (13) (a) Kräusslich, H. G.; Fäcke, M.; Heuser, A. M.; Konvalinka, J.; Zentgraf, H. The spacer peptide between human immunodeficiency virus capsid and nucleocapsid proteins is essential for ordered assembly and viral infectivity. *J. Virol.* **1995**, *69*, 3407-3419. (b) Accola, M. A.; Höglund, S.; Göttinger, H. G. A putative alpha-helical structure which overlaps the capsid-P2 boundary in the human immunodeficiency virus type 1 Gag precursor is crucial for viral particle assembly. *J. Virol.* **1998**, *72*, 2072-2078.

- (14) (a) Pettit, S. C.; Henderson, G. J.; Schiffer C. A; Swanstrom, R. Replacement of the P1 amino acid of HIV-1 Gag processing sites can inhibit or enhance the rate of cleavage by the viral protease. *J. Virol.* **2002**, 76, 10226-10233. (b) Wiegers, K.; Rutter, G.; Kottler, H.; Tessmer, U.; Hohenberg, H.; Krausslich, H.-G. Sequential steps in human immunodeficiency virus particle maturation revealed by alterations of individual Gag polyprotein cleavage sites. *J. Virol.* **1998**, 72, 2846-2854.
- (15) Freed, E. O. HIV-1 assembly, release and maturation. *Nat. Rev. Microbiol.* **2015**, 13, 484–496.
- (16) (a) Martin, D. E.; Salzwedel, K.; Allaway, G. P. Bevirimat: a novel maturation inhibitor for the treatment of HIV-1 infection. *Antiviral Chem. Chemother.* **2008**, 19, 107-113. (b) Salzwedel, K.; Martin, D. E.; Sakalian, M. Maturation inhibitors: a new therapeutic class targets the virus structure. *AIDS Rev.* **2007**, 9, 162-172. (c) Temesgen, Z.; Feinberg, J. E. Drug evaluation: bevirimat - HIV Gag protein and viral maturation inhibitor. *Curr. Opin. Investig. Drugs* **2006**, 7, 759-765. (d) Wang, D.; Lu, W.; Li, F. Pharmacological intervention of HIV-1 maturation. *Acta Pharm. Sin. B.* [Online early access]. DOI:10.1016/j.apsb.2015.05004. Published Online: June 11, **2015**.
- (17) Smith, P.F.; Ogundele, A.; Forrest, J. W.; Salzwedel, K.; Doto, J.; Allaway, G. P.; Martin, D. E. Phase I and II study of the safety, virologic effect, and pharmacokinetics / pharmacodynamics of single-dose 3-*O*-(3'-dimethylsuccinyl)betulinic acid (bevirimat) against human immunodeficiency virus infection. *Antimicrob. Agents Chemother.* **2007**, 51, 3574-3581.
- (18) (a) McCallister, S.; Lalezari, J.; Richmond, G.; Thompson, M.; Harrigan, R.; Martin, D.; Salzwedel, K.; Allaway, G. HIV-1 Gag polymorphisms determine treatment response to bevirimat (PA-457). *Antiviral Ther.* **2008**, 13:A10. (b) Baelen, K. V.; Salzwedel, K.;

- Rondelez, E.; Veerle Van Eygen, V. V.; De Vos, S.; Verheyen, A.; Steegen, K.; Verlinden, Y.; Allaway, G. P.; Stuyver, L. J. Susceptibility of human immunodeficiency virus type 1 to the maturation inhibitor bevirimat is modulated by baseline polymorphisms in Gag spacer peptide 1. *Antimicrob. Agents Chemother.* **2009**, *53*, 2185-2188; (c) Margot, N. A.; Gibbs, C. S.; Miller, M. D. Phenotypic susceptibility to bevirimat among HIV-1 infected patient isolates without prior exposure to bevirimat. *Antimicrob. Agents Chemother.* **2010**, *54*, 2345-2353.
- (19) Kilgore, N.; Reddick, M.; Zuiderhof, M.; Stanley, D.; Nitz, T.; Bullock, P.; Allaway, G.; Martin, D. Characterization of PA1050040, a second generation HIV-1 maturation inhibitor. Poster discussion: *4th IAS Conference on HIV Pathogenesis, Treatment and Prevention*. Sydney, Australia July 22-25, **2007**. Abstract no. MOPDX05.
- (20) Jacob, J.; Richards, J.; Augustine, J. G.; Milea, J. S.; Liquid bevirimat dosage forms for oral administration. *World Patent Application*, WO 2009/042166 A1. November 5, **2009**.
- (21) Albert, J. Can the further clinical development of bevirimat be justified? *AIDS* **2010**, *24*, 773-774.
- (22) Kashiwada, Y.; Hashimoto, F.; Cosentino, L. M.; Chen, C.; Garrett, P. E.; Lee, K.-H. Betulinic acid and dihydrobetulinic acid derivatives as potent anti-HIV agents. *J. Med. Chem.* **1996**, *39*, 1016-1017.
- (23) Dang, Z.; Ho, P.; Zhu, L.; Qian, K.; Lee, K.-H.; Huang, L.; Chen, C.-H. New betulinic acid derivatives for bevirimat-resistant human immunodeficiency virus type-1. *J. Med. Chem.* **2013**, *56*, 2029-2037.
- (24) (a) Qian, K.; Bori, I. D.; Chen, C. H.; Huang, L.; Lee, K. H. Anti-AIDS agents 90. Novel C-28 modified bevirimat analogs as potent HIV maturation inhibitors. *J. Med. Chem.* **2012**, *55*, 8128-8136. (b) Urano, E.; Ablan, S. D.; Mandt, R.; Pauly, G. T.; Sigano, D. M.; Scheneider, J. P.; Martin, D. E.; Nitz, T. J.; Wild, C. T.; Freed, E. O. Alkyl amine bevirimat derivatives are

potent and broadly active HIV-1 Maturation Inhibitors. *Antimicrob. Agents Chemother.* [Online early access]. DOI: 10.1128/AAC.02121-15. Posted Online: 19 October 2015.

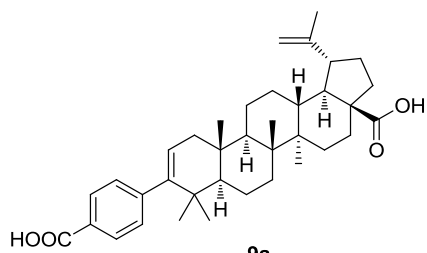
- (25) (a) Kashiwada, Y.; Chiyo, J.; Ikeshiro, Y.; Nagao, T.; Okabe, H.; Cosentino, H. L.; Fowke, K.; Morris-Natschke, S. L.; Lee, K.-H. Synthesis and anti-HIV activity of 3-alkylamido-3-deoxy-betulinic acid derivatives. *Chem. Pharm. Bull.* **2000**, 48, 1387-1390. (b) Qian, K.; Nakagawa-Goto, K.; Yu, D.; Morris-Natschke, S. L.; Nitz, T. J.; Kilgore, N.; Allaway, G. P.; Lee, K.-H. Anti-AIDS agents 73: structure-activity relationship study and asymmetric synthesis of 3-*O*-methylsuccinyl-betulinic acid derivatives. *Bioorg. Med. Chem. Lett.* **2007**, 17, 6553-6557.
- (26) Jung, M. E.; Pizzi, G. Gem-disubstituent effect: theoretical basis and synthetic applications *Chem. Rev.* **2005**, 105, 1735-1766.
- (27) Sun, I.-C.; Shen, J.-K.; Wang, H.-K.; Cosentino, L. M.; Lee, K.-H. Anti-AIDS agents. 32. Synthesis and anti-HIV activity of betulin derivatives. *Bioorg. Med. Chem. Lett.* **1998**, 8, 1267-1272.
- (28) (a) Kashiwada, Y.; Nagao, T.; Hashimoto, A.; Ikeshiro, Y.; Okabe, H.; Cosentino, L. M.; Lee, K.-H. Anti-AIDS agents 38. Anti-HIV activity of 3-*O*-acyl ursolic acid derivative. *J. Nat Prod* **2000**, 63, 1619-1622. (b) Yu, D.; Sakurai, Y.; Chen, C.-H.; Chang, F.-R.; Huang, L.; Kashiwada, Y.; Lee, K.-H. Anti-AIDS agents 69. Moronic acid and other triterpene derivatives as novel potent anti-HIV agents. *J. Med. Chem.* **2006**, 49, 5462-5469.
- (29) Qian, K.; Kuo, R.-Y.; Chen, C.-H.; Huang, L.; Morris-Natschke, S. L.; Lee, K.-H. Anti-AIDS agents 81. Design, synthesis and structure-activity relationship study of betulinic acid and moronic acid derivatives as potent HIV maturation inhibitors. *J. Med. Chem.* **2010**, 53, 3133-3341.

- (30) Hwang, C.; Schürmann, D.; Shobotha, C.; Sevinsky, H.; Ravindran, P.; Xiao, H.; Ray, N.; Krystal, M.; Dicker, I. B.; Lataillade, M. Antiviral activity/safety of a second generation HIV-1 maturation inhibitor. *22nd Conference on Retroviruses and Opportunistic Infections*, Seattle, WA. February 23-26, **2015**. Abstract #114LB.
- (31) Regueiro-Ren, A.; Swidorski, J. Liu, Z.; Meanwell, N. A.; Sit, S.; Chen, J.; Sin, N. Modified C-3 betulinic acid derivatives as HIV maturation inhibitors. U.S. Patent 8,754,068, June 17, **2014**.
- (32) Nowicka-Sans B.; Protack, T.; Lin, Z.; Li, Z.; Zhang, S.; Samanta H.; Terry, B.; Liu, Z.; Chen, Y.; Sin N.; Sit, S.-Y.; Swidorski, J. J.; Chen, J.; Venables, B. L.; Healy, M.; Sun, Y.; Meanwell, N. A.; Cockett, M.; Hanumegowda, U.; Regueiro-Ren, A.; Krystal, M.; Dicker, I. B. BMS-955176: Identification and characterization of a second-generation HIV 1 maturation inhibitor with improved potency, anti-viral spectrum and Gag polymorphic coverage. *Antimicrob. Agents Chemother.*, Manuscript accepted.
- (33) <http://www.hiv.lanl.gov/content/sequence/NEWALIGN/align.html#filter>
- (34) Tominaga, H.; Ishiyama, M.; Ohseto, F.; Sasamoto, K.; Hamamoto, T.; Suzuki, K.; Watanabe, M. A water-soluble tetrazolium salt useful for colorimetric cell viability assay. *Analytical Communications* **1999**, 36 47-50.
- (35) Banks, J. L.; Beard, H. S.; Cao, Y.; Cho, A. E.; Damm, W.; Farid, R.; Felts, A. K.; Halgren, T. A.; Mainz, D. T.; Maple, J. R.; Murphy, R.; Philipp, D. M.; Repasky, M. P.; Zhang, L. Y.; Berne, B. J.; Friesner, R. A.; Gallicchio, E.; Levy, R. M. Integrated modeling program, applied theory (IMPACT). *J. Comp. Chem.* **2005**, 26, 1752-1780.
- (36) (a) Herr, J. R. 5-Substituted 1H-tetrazoles as carboxylic acid isosteres: medicinal chemistry and synthetic methods. *Bioorg. Med. Chem.* **2002**, 10, 3379-3393. (b) Meanwell, N. A. Synopsis of some recent tactical applications of bioisosteres in drug design. *J. Med. Chem.*

- 2011**, 54, 2529–2591. (c) Matta, C. F.; Arabi, A. A.; Weaver, D. F. The bioisosteric similarity of the tetrazole and carboxylate anions: clues from the topologies of the electrostatic potential and of the electron density. *Eur. J. Med. Chem.* **2010**, 45, 1868–1872. (d) Allen, F. H.; Groom, C. R.; Liebeschuetz, J. W.; Bardwell, D. A.; Olsson, T. S. G.; Wood, P. A. The hydrogen bond environments of 1*H*-tetrazole and tetrazolate rings: the structural basis for tetrazole-carboxylic acid bioisosterism. *J. Chem. Inf.* **2012**, 52, 857–866. (e) Ballatore, C.; Huryn, D. M.; Smith, A. B., 3rd. Carboxylic acid (bio)isosteres in drug design. *ChemMedChem* **2013** 8, 385-395.
- (37) Firestine, S. M.; Davisson, V. J. A tight binding inhibitor of 5-aminoimidazole ribonucleotide carboxylase. *J. Med. Chem.* **1993**, 36, 3484-3486.
- (38) Scola, P. M.; Sun, L.; Wang, A. X.; Chen, J.; Sin, N.; Venables, B. L.; Sit, S.; Chen, Y.; Cocuzza, A.; Bilder, D. M.; D'Andrea, S. V.; Zheng, B.; Hewawasam, P.; Tu, Y.; Friborg, J.; Falk, P.; Hernandez, D.; Levine, S.; Chen, C.; Yu, F.; Sheaffer, A. K.; Zhai, G.; Barry, D.; Knipe, J. O.; Han, Y.; Schartman, R.; Donoso, M.; Mosure, K.; Sinz, M. W.; Zvyaga, T.; Good, A. C.; Rajamani, R.; Kish, K.; Tredup, J.; Klei, H. E.; Gao, Q.; Mueller, L.; Colonno, R. J.; Grasela, D. M.; Adams, S. P.; Loy, J.; Levesque, P. C.; Sun, H.; Shi, H.; Sun, L.; Warner, W.; Li, D.; Zhu, J.; Meanwell, N. A.; McPhee, F. The discovery of asunaprevir (BMS-650032), an orally efficacious NS3 protease inhibitor for the treatment of hepatitis C virus infection. *J. Med. Chem.* **2014**, 57, 1730–1725.
- (39) Eliel, E. L.; Allinger, N. L.; Angyal, S. J.; Morrison, G. A. *Conformational Analysis*. Interscience Publishers: New York, 1965.
- (40) Pettit, S. C.; Lindquist, J. N.; Kaplan, A. H.; Swanstrom, R. Processing sites in the human immunodeficiency virus type 1 (HIV-1) Gag-Pro-Pol precursor are cleaved by the viral protease at different rates. *Retrovirology*, **2005**, 2, 66-71.

- (41) Zhou, J. X.; Yuan, D.; Dismuke, D.; Forshey, B. M.; Lundquist, C.; Lee, K.-H.; Aiken, C.; Chen, C. H. Small-molecule inhibition of human immunodeficiency virus type 1 replication by specific targeting of the final step of virion maturation. *J. Virol.* **2004**, 78, 922-929.
- (42) Lin, Z.; Cantone, J.; Protack, T.; Drexler, D.; Nowicka-Sans, B.; Tian, Y.; Liu, Z.; Krystal, M.; Regueiro-Ren, A.; Dicker, I. B. Maturation inhibitor mechanistic studies - understanding and modelling differential inhibition of Gag polymorphs. *22nd Conference on Retroviruses and Opportunistic Infections*, Seattle, WA. February 23-26, **2015**; Abstract #539.
- (43) Fujioka, T.; Kashiwada, Y.; Kilkuskie, R. E.; Cosentino, L. M.; Ballas, L. M.; Jiang, J. B.; Janzen, W. P.; Chen, I. S.; and Lee, K. H. *J. Nat. Prod.* **1994**, 57, 243-247.
- (44) Nowicka-Sans B.; Protack, T.; Lin, Z.; Li, Z.; Zhang, S.; Meanwell, N. A.; Cockett, M.; Regueiro-Ren, A.; Krystal, M.; Dicker. BMS-955176: Characterization of a second-generation HIV 1 maturation inhibitor. *8th IAS Conference on HIV Pathogenesis, Treatment and Prevention*, Vancouver, Canada, July 19-22, **2015**; poster: TUPEA078.
- (45) Johnson, V. A.; Byington, A.; Walker, B. D. Infectivity assay, in techniques in HIV research. Walker, B. D., Editor. Stockton Press: New York, NY, **1990**, p. 1-76.

Graphical abstract



9a
WT EC_{50} = 0.016 μ M
V370A = 0.233 μ M
WT (15 mg/mL HSA) = 0.105 μ M